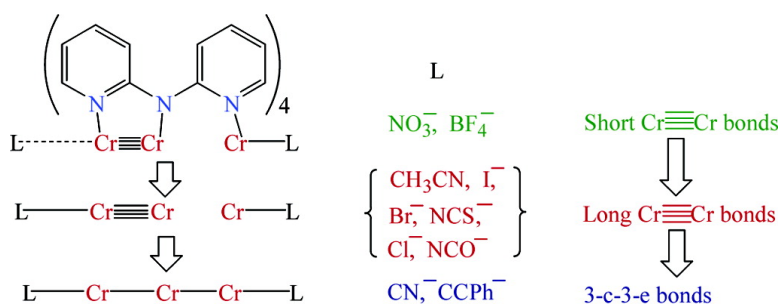


Molecular and Electronic Structures by Design: Tuning Symmetrical and Unsymmetrical Linear Trichromium Chains

John F. Berry, F. Albert Cotton, Tongbu Lu, Carlos A. Murillo, Brian K. Roberts, and Xiaoping Wang

J. Am. Chem. Soc., **2004**, 126 (22), 7082-7096 • DOI: 10.1021/ja049055h • Publication Date (Web): 14 May 2004

Downloaded from <http://pubs.acs.org> on March 31, 2009



More About This Article

Additional resources and features associated with this article are available within the HTML version:

- Supporting Information
- Links to the 7 articles that cite this article, as of the time of this article download
- Access to high resolution figures
- Links to articles and content related to this article
- Copyright permission to reproduce figures and/or text from this article

[View the Full Text HTML](#)



ACS Publications
 High quality. High impact.

Molecular and Electronic Structures by Design: Tuning Symmetrical and Unsymmetrical Linear Trichromium Chains

John F. Berry,[†] F. Albert Cotton,^{*,†} Tongbu Lu,^{†,‡} Carlos A. Murillo,^{*,†}
Brian K. Roberts,^{†,§} and Xiaoping Wang[†]

Contribution from the Department of Chemistry and Laboratory for Molecular Structure and Bonding, P.O. Box 30012, Texas A&M University, College Station, Texas 77842-3012, School of Chemistry & Chemical Engineering, Sun Yat-Sen University, Guangzhou 510275, P. R. China, and Department of Chemistry, Florida State University, Tallahassee, Florida 32306

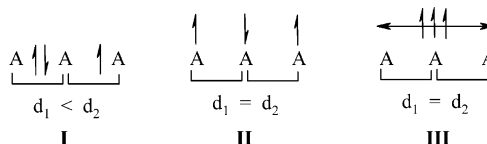
Received February 19, 2004; E-mail: cotton@tamu.edu; murillo@tamu.edu

Abstract: The preparation, properties, and crystal structures of 12 trichromium extended metal atom chain (EMAC) compounds of the type $\text{Cr}_3(\text{L})_4\text{X}_2$ (L = equatorial ligands dipyritylamide (dpa) or di-4,4'-ethyl-2,2'-pyridylamide (depa), and X = axial ligands, e.g., halide or pseudohalide ions) with large variations in metal-metal distances are reported here. These complexes, which belong to a broad class of fundamentally interesting trinuclear molecules over which the electrons may or may not be delocalized, pose significant theoretical and experimental challenges which are dealt with in this report. Complexes with strongly donating axial or equatorial ligands tend to favor a symmetrical (D_4) molecular structure, while more weakly donating ligands give rise to unsymmetrical (C_4) structures; the physical properties of these two classes of compounds are discussed fully, and important comparisons with a reported DFT model of the electronic structures of the compounds are made.

1. Introduction

Delocalized multicenter bonding in polyatomic systems poses significant challenges to molecular quantum mechanics.¹ Trinuclear molecules or ions are the most fundamental examples of a broad class of polyatomics which contain species such as I_3^- ,² alkali³ or coinage⁴ metal trimers, carbon-rich chains⁵ such as the allyl radical,⁶ O_3 ,⁷ and the recently synthesized⁸ N_5^+ cation,⁹ among others.¹⁰ Despite their simplicity, these entities tend not to be structurally rigid. For example, systems with three

Scheme 1



electrons (Scheme 1) can be either localized having a doublet ground state with unequal (**I**) or equal (**II**) interatomic distances, or delocalized (**III**) having equal interatomic distances. In the latter, the three electrons are in orbitals spanning all three atoms, and these can be either paired or unpaired.

[†] Texas A&M University.

[‡] Sun Yat-Sen University.

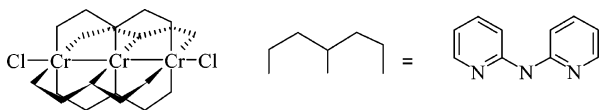
[§] Florida State University.

- (1) (a) Munzarová, M. L.; Hoffmann, R. *J. Am. Chem. Soc.* **2002**, *124*, 4787. (b) Macchi, P.; Sironi, A. *Coord. Chem. Rev.* **2003**, *238*, 383. (c) Harcourt, R. D. *J. Phys. Chem. A* **1999**, *103*, 4293. (d) Harcourt, R. D. *J. Phys. Chem. A* **2003**, *107*, 11260. (e) Ramsden, C. A. *Chem. Soc. Rev.* **1994**, *111*. (f) Vela, A.; Merino, G. *Rev. Mod. Quantum Chem.* **2002**, *2*, 1140. (g) Rasul, G.; Olah, G. A.; Prakash, G. K. S. *Inorg. Chem.* **2003**, *42*, 8059. (h) Kar, T.; Angyán, J. G.; Sannigrahi, A. B. *J. Phys. Chem. A* **2000**, *104*, 9953. (i) Alkorta, I.; Abboud, J. L. M.; Quintanilla, E.; Dávalos, J. Z. *J. Phys. Org. Chem.* **2003**, *16*, 564. (j) Harcourt, R. D. *J. Mol. Struct. (THEOCHEM)* **2002**, *617*, 177. (k) Sannigrahi, A. B.; Kar, T. *J. Mol. Struct. (THEOCHEM)* **2000**, *496*, 1. (l) Shaik, S.; Shurki, A.; Danovich, D.; Hiberty, P. C. *Chem. Rev.* **2001**, *101*, 1501. (m) Jug, K.; Hiberty, P. C.; Shaik, S. *Chem. Rev.* **2001**, *101*, 1477.
- (2) (a) Svensson, P. H.; Kloo, L. *J. Chem. Soc., Dalton Trans.* **2000**, *14*, 2449. (b) Margulis, C. J.; Coker, D. F.; Lynden-Bell, R. M. *Chem. Phys. Lett.* **2001**, *341*, 557. (c) Koslowski, T.; Vöhringer, P. *Chem. Phys. Lett.* **2001**, *342*, 141. (d) Kloo, L.; Rosdahl, J.; Svensson, P. H. *Eur. J. Inorg. Chem.* **2002**, *1203*. (e) Lin, Z.; Hall, M. B. *Polyhedron* **1993**, *12*, 1499. (f) Vala, J.; Kosloff, R.; Harvey, J. N. *J. Chem. Phys.* **2001**, *114*, 7413. (g) Margulis, C. J.; Coker, D. F.; Lynden-Bell, R. M. *J. Chem. Phys.* **2001**, *114*, 367. (h) Sato, H.; Hirata, F.; Myers, A. B. *J. Phys. Chem. A* **1998**, *102*, 2065. (i) Zhang, F. S.; Lynden-Bell, R. M. *Phys. Rev. Lett.* **2003**, *90*, 185505-1. (j) Gorinchoi, N. N.; Cimpoesu, F.; Bersuker, I. B. *J. Mol. Struct. (THEOCHEM)* **2000**, *530*, 281.
- (3) (a) Martins, J. L.; Car, R.; Buttet, J. *J. Chem. Phys.* **1983**, *78*, 5646. (b) Malrieu, J. P. *Nouv. J. Chim.* **1986**, *10*, 61.
- (4) Berthier, G.; Barthelat, J. C.; Dangeard, I.; Tao, Y. *J. Phys.-Chim. Biol.* **1987**, *84*, 677.
- (5) (a) Brown, L. D.; Lipscomb, W. N. *J. Am. Chem. Soc.* **1977**, *99*, 3968. (b) Siddarth, P.; Gopinathan, M. S. *J. Am. Chem. Soc.* **1988**, *110*, 96. (c) Ohno, M.; Zakrzewski, V. G.; Ortiz, J. V.; von Niessen, W. *J. Chem. Phys.* **1997**, *106*, 3258. (d) Ortiz, J. V.; Zakrzewski, V. G. *J. Chem. Phys.* **1994**, *100*, 6614. (e) Hiberty, P. C.; Ohanessian, G.; Shaik, S. S.; Flament, J. P. *Pure Appl. Chem.* **1993**, *65*, 35.
- (6) (a) Shaik, S. S.; Hiberty, P. C.; Ohanessian, G.; Lefour, J. M. *J. Phys. Chem.* **1988**, *92*, 5086. (b) Shaik, S. S.; Hiberty, P. C.; Ohanessian, G.; Lefour, J. M. *Nouv. J. Chim.* **1985**, *9*, 385. (c) Shaik, S. S.; Hiberty, P. C.; Lefour, J. M.; Ohanessian, G. *J. Am. Chem. Soc.* **1987**, *109*, 363. (d) Berthier, G. *Can. J. Chem.* **1985**, *63*, 1681.
- (7) (a) Laing, M. *Struct. Chem.* **1995**, *6*, 397. (b) Laing, M. *Educ. Chem.* **1996**, *46*.
- (8) Christe, K. O.; Wilson, W. W.; Sheehy, J. A.; Boatz, J. A. *Angew. Chem., Int. Ed.* **1999**, *38*, 2004.
- (9) (a) Netzloff, H. M.; Gordon, M. S.; Chroste, K.; Wilson, W. W.; Vij, A.; Vij, V.; Boatz, J. A. *J. Phys. Chem. A* **2003**, *107*, 6638. (b) Fau, S.; Wilson, K. J.; Bartlett, R. J. *J. Phys. Chem. A* **2002**, *106*, 4639. (c) Kerkines, I. S. K.; Papakondylis, A.; Mavridis, A. *J. Phys. Chem. A* **2002**, *106*, 4453. (d) Wang, L. J.; Qian, S. L.; Warburton, P.; Mezey, P. G. *J. Phys. Chem. A* **2002**, *106*, 1872. (e) Ponec, R.; Roithová, J.; Gironés, X.; Jug, K. *J. Mol. Struct. (THEOCHEM)* **2001**, *545*, 255. (f) Harcourt, R. D.; Klapötke, T. M. *Z. Naturforsch.* **2002**, *57*, 983. (g) Harcourt, R. D.; Klapötke, T. M. *Z. Naturforsch.* **2003**, *58*, 121.
- (10) (a) Schuh, W.; Braunstein, P.; Bénard, M.; Rohmer, M.-M.; Welter, R. *Angew. Chem., Int. Ed.* **2003**, *42*, 2161. (b) Shaik, S. S.; Bar, R. *Inorg. Chem.* **1983**, *22*, 735. (c) Xu, L.; Ugrinov, A.; Sevov, S. C. *J. Am. Chem. Soc.* **2001**, *123*, 4091.

Polynuclear systems having metal–metal multiple bonds have also been of considerable interest both to experimentalists and theorists.¹¹ The simpler dinuclear systems have been extensively studied, and in many cases the electronic structure is well understood,¹¹ an exception being those with quadruply bonded Cr_2^{4+} units. Many compounds of this type have been prepared,¹² and they exhibit a wide variation of Cr–Cr bond distances ranging from 1.83 to ~ 2.6 Å. These are essentially diamagnetic¹³ and are described as having a formal Cr–Cr quadruple bond. The reason for this remarkable variability of Cr–Cr bond lengths is that axial donors L destabilize the Cr–Cr σ bond through either σ^{14} or π^{15} interactions. These chromium compounds have presented major challenges from a theoretical standpoint,¹⁶ and reliable calculations on Cr_2^{4+} complexes have been difficult to obtain due to electron correlation effects.¹⁷ Nevertheless, the description of Cr_2^{4+} compounds as having a $\sigma^2\pi^4\delta^2$ configuration has been helpful, if not a totally correct approximation,¹¹ and it has permitted an explanation of the geometry and electronic structure and those of a recently synthesized Cr_2^{5+} cationic unit.¹⁸

In 1997, this laboratory reported the first compounds with metal–metal bonded units forming extended metal atom chains (EMACs) of three Cr(II) atoms, the prototype being $\text{Cr}_3(\text{dpa})_4\text{Cl}_2$ (**1**, dpa is the anion of di-2,2'-pyridylamine, see Scheme 2).¹⁹

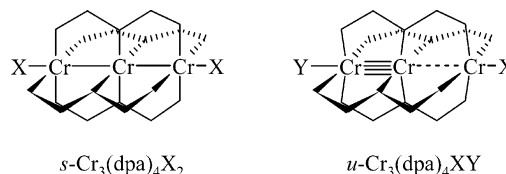
Scheme 2



In subsequent work with trichromium complexes of this type, we found that in some cases the Cr–Cr distances were equal, but in others a rather unsymmetrical Cr_3 chain exists.²⁰ This prompted us to consider **1** as existing as a pair of bond stretch isomers: two compounds (symmetrical-**1** and

unsymmetrical-**1**) which are different only by the length of one or more bonds.²¹ The analogous tricobalt compound, $\text{Co}_3(\text{dpa})_4\text{Cl}_2$, unequivocally exists in two different and well-characterized forms, *s*- $\text{Co}_3(\text{dpa})_4\text{Cl}_2$ and *u*- $\text{Co}_3(\text{dpa})_4\text{Cl}_2$, which fit the description of bond stretch isomers.²² For chromium complexes of the type $\text{Cr}_3(\text{dpa})_4\text{XY}$, symmetrical chains were reported when $X = Y$, but when $X \neq Y$ the Cr–Cr distances become so different that the Cr_3^{6+} chain could be described as consisting of a diamagnetic Cr_2^{4+} quadruply bonded unit tethered to a high-spin Cr(II) ion at a nonbonding distance (see Scheme 3).²³ Both symmetrical and unsymmetrical compounds

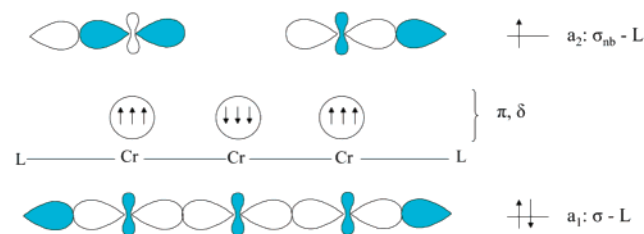
Scheme 3



have $S = 2$ ground states. This is in contrast to $\text{Co}_3(\text{dpa})_4\text{Cl}_2$ for which the symmetrical and unsymmetrical “isomers” have qualitatively different magnetic properties inter alia.²²

To help explain the experimental findings, DFT calculations have been carried out by Bénard, Rohmer, and co-workers on the parent complex $\text{Cr}_3(\text{dpa})_4\text{Cl}_2$.²⁴ According to these calculations, there is a symmetrical ground state with $d_{\text{Cr–Cr}} = 2.350$ Å. This was rationalized in terms of a 3-center-3-electron bond consisting of a filled 3-center σ bonding orbital and a half-filled σ nonbonding orbital. The remaining 9 Cr-based electrons are localized on the three Cr atoms in orbitals of π and δ symmetry and couple antiferromagnetically and very strongly to produce the observed $S = 2$ ground state shown in Scheme 4. The relative energies of the σ and σ_{nb} orbitals are influenced

Scheme 4



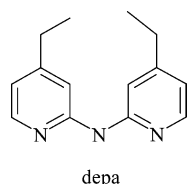
by destabilizing interactions with the axial ligands.

Although a very unsymmetrical structure for $\text{Cr}_3(\text{dpa})_4\text{Cl}_2$ (e.g., with $\Delta d_{\text{Cr–Cr}} = 0.679$ Å) was calculated to lie >4 kcal mol^{-1} above the symmetrical ground state, it was postulated that an unsymmetrical set of axial ligands could stabilize such a state, which rationalizes the very unsymmetrical structures of $\text{Cr}_3(\text{dpa})_4(\text{BF}_4)\text{Cl}$ and $\text{Cr}_3(\text{dpa})_4(\text{PF}_6)\text{Cl}$.²⁵ Intermediate geometries with $\Delta d_{\text{Cr–Cr}} \approx 0.1$ Å were calculated to lie <1 kcal mol^{-1} above the ground state,²⁴ and thus the energy required to move the central Cr atom toward one of the two terminal Cr atoms is quite small, and about the same order of magnitude as kT .

- (11) Cotton, F. A.; Walton, R. A. *Multiple Bonds Between Metal Atoms*, 2nd ed.; Oxford University Press: New York, 1993.
- (12) (a) Cotton, F. A.; Murillo, C. A.; Pascual, I. *Inorg. Chem.* **1999**, *38*, 2182. (b) Cotton, F. A.; Daniels, L. M.; Murillo, C. A.; Schooler, P. *J. Chem. Soc., Dalton Trans.* **2000**, 2007. (c) Hao, S.; Gambarotta, S.; Bensimon, C.; Edema, J. J. H. *Inorg. Chim. Acta* **1993**, *213*, 65. (d) Cotton, F. A.; Daniels, L. M.; Murillo, C. A.; Schooler, P. *J. Chem. Soc., Dalton Trans.* **2000**, 2001. (e) Carlton-Day, K. M.; Eglin, J. L.; Lin, C.; Smith, L. T.; Staples, R. J.; Wipf, D. O. *Polyhedron* **1999**, *18*, 817. (f) Dionne, M.; Hao, S.; Gambarotta, S. *Can. J. Chem.* **1995**, *73*, 1126. (g) Cotton, F. A.; Timmons, D. J. *Polyhedron* **1998**, *17*, 179. (h) Mashima, K.; Tanaka, M.; Tani, K.; Nakamura, A.; Tadeka, S.; Mori, W.; Yamaguchi, K. *J. Am. Chem. Soc.* **1997**, *119*, 4307.
- (13) In some cases, weak paramagnetism is observed for Cr_2^{4+} species due to the partial population of an excited triplet state, although the ground state has $S = 0$. See: Cotton, F. A.; Chen, H.; Daniels, L. M.; Feng, X. *J. Am. Chem. Soc.* **1992**, *114*, 8980.
- (14) Cotton, F. A.; Hillard, E. A.; Murillo, C. A.; Zhou, H.-C. *J. Am. Chem. Soc.* **2000**, *122*, 416.
- (15) Cotton, F. A.; Daniels, L. M.; Murillo, C. A.; Pascual, I.; Zhou, H.-C. *J. Am. Chem. Soc.* **1999**, *121*, 6856.
- (16) (a) Ponc, R.; Yuzhakov, G.; Carbó-Dorca, R. *J. Comput. Chem.* **2003**, *24*, 1829. (b) Lichtenberger, D. L.; Lynn, M. A.; Chisholm, M. H. *J. Am. Chem. Soc.* **1999**, *121*, 12167. (c) Nishino, M.; Yamanaka, S.; Yoshioka, Y.; Yamaguchi, K. *J. Phys. Chem. A* **1997**, *101*, 705. (d) Nishino, M.; Yoshioka, Y.; Yamaguchi, K.; Mashima, K.; Tani, K.; Nakamura, A. *Bull. Chem. Soc. Jpn.* **1998**, *71*, 99. (e) Andersson, K.; Bauschlicher, C. W., Jr.; Persson, B. J.; Roos, B. O. *Chem. Phys. Lett.* **1996**, *257*, 238.
- (17) Hall, M. B. *Polyhedron* **1987**, *6*, 679.
- (18) (a) Cotton, F. A.; Daniels, L. M.; Huang, P.; Murillo, C. A. *Inorg. Chem.* **2002**, *41*, 317. (b) Cotton, F. A.; Dalal, N. S.; Hillard, E. A.; Huang, P.; Murillo, C. A.; Ramsey, C. M. *Inorg. Chem.* **2003**, *42*, 1388.
- (19) Cotton, F. A.; Daniels, L. M.; Murillo, C. A.; Pascual, I. *J. Am. Chem. Soc.* **1997**, *119*, 10223.
- (20) Cotton, F. A.; Daniels, L. M.; Murillo, C. A.; Pascual, I. *Inorg. Chem. Commun.* **1998**, *1*, 1.

- (21) Parkin, G. *Acc. Chem. Res.* **1992**, *25*, 455.
- (22) Clérac, R.; Cotton, F. A.; Daniels, L. M.; Dunbar, K. R.; Kirschbaum, K.; Murillo, C. A.; Pinkerton, A. A.; Schultz, A. J.; Wang, X. *J. Am. Chem. Soc.* **2000**, *122*, 6226.
- (23) Clérac, R.; Cotton, F. A.; Daniels, L. M.; Dunbar, K. R.; Murillo, C. A.; Pascual, I. *Inorg. Chem.* **2000**, *39*, 748.
- (24) Benbellat, N.; Rohmer, M.-M.; Bénard, M. *Chem. Commun.* **2001**, 2368.
- (25) Rohmer, M.-M.; Bénard, M. *J. Cluster Sci.* **2002**, *13*, 333.

Scheme 5



We began this work to provide some insight into the factors which are ultimately responsible for the appearance of a symmetrical versus an unsymmetrical Cr_3^{6+} chain in the solid state and to see if the molecular geometry could be tuned by changing the electronic effects of the axial and equatorial ligands. We also wanted to see if it was possible to find more conclusive evidence either for or against **1** forming bond stretch isomers. During the course of this work, we found it necessary to reexamine some of our previously reported results on $\text{Cr}_3(\text{dpa})_4\text{Cl}_2$,²³ as well as to synthesize new compounds with various axial donor ligands and Cr_3^{6+} and Cr_3^{7+} compounds stabilized by the substituted depa (i.e., the anion of di-4,4'-ethyl-2,2'-pyridylamine) equatorial ligand (see Scheme 5).

The compounds are as follows: $\text{Cr}_3(\text{dpa})_4\text{Cl}_2$, **1**; $\text{Cr}_3(\text{depa})_4\text{Cl}_2$, **2**; $[\text{Cr}_3(\text{depa})_4\text{Cl}_2]\text{I}_3$, **3**; $[\text{Cr}_3(\text{dpa})_4(\text{NCCH}_3)_2](\text{PF}_6)_2$, **4**; $\text{Cr}_3(\text{dpa})_4\text{I}_2$, **5**; $\text{Cr}_3(\text{dpa})_4\text{Br}_2$, **6**; $\text{Cr}_3(\text{dpa})_4(\text{NO}_3)_2$, **7**; $\text{Cr}_3(\text{dpa})_4(\text{BF}_4)_2$, **8**; $\text{Cr}_3(\text{dpa})_4(\text{CN})_2$, **9**; $\text{Cr}_3(\text{dpa})_4(\text{NCS})_2$, **10**; $\text{Cr}_3(\text{dpa})_4(\text{NCO})_2$, **11**; and $[\text{Cr}_3(\text{dpa})_4(\text{NCO})\text{F}]\text{PF}_6$, **12**. Further work on $\text{Cr}_3(\text{dpa})_4(\text{CCPh})_2$, **13**, is also reported.

The results of this work are relevant to the areas of metal–metal bonding¹¹ and molecular electronics,²⁶ since changes in molecular geometries that will either enhance or diminish delocalized metal–metal bonding are of utmost importance to the design of useful molecular switches. The possibility of switching the molecular structure of a trichromium compound such as **1** from symmetrical to unsymmetrical through an outside source such as an applied potential comes to mind. Moreover, compounds which can behave electronically as switches are useless if they cannot be integrated into a circuit. So, we report our exploration of the chemistry of $\text{Cr}_3(\text{dpa})_4\text{X}_2$ compounds and methods for varying the X anions which should be applicable to a variety of X ligands.

2. Experimental Section

General. All manipulations were carried out under dry nitrogen using standard Schlenk techniques. THF, ether, dichloromethane, hexanes, toluene, and benzene were purified using a Glass Contour system. All other solvents were distilled in a nitrogen atmosphere over appropriate drying agents prior to use, and reagents available from commercial sources were used as received unless otherwise specified. $\text{Cr}_3(\text{dpa})_4\text{Cl}_2$, **1**, was prepared as reported previously.²³ The ligand Hdepa was synthesized as published.²⁷ Commercial grade anhydrous CrCl_2 was refluxed in Me_3SiCl prior to use. Thallium hexafluorophosphate, KCN, NaI, KBr, TlNO_3 , NaNCO , and KSCN were dried overnight under dynamic vacuum at 80 °C prior to use. $\text{Cr}_3(\text{dpa})_4(\text{CCPh})_2$, **13**, was prepared according to a published procedure.²⁸ Thallium tetrafluoroborate was prepared from TlCO_3 and HBF_4 in ether and dried overnight

at 80 °C under vacuum prior to use. Ferrocenium triiodide was prepared by mixing hexanes solutions of appropriate amounts of ferrocene and I_2 .²⁹

Physical Measurements. The IR spectra were taken on a Perkin-Elmer 16PC FTIR spectrometer using KBr pellets. Cyclic voltammograms were taken on a CH Instruments electrochemical analyzer using dichloromethane solutions with 1 M NBu_4PF_6 and 0.1 mM analyte. The electrodes were as follows: Pt disk (working), Pt wire (auxiliary), and Ag/AgCl (reference). Elemental analyses were carried out by Canadian Microanalytical Services in British Columbia, Canada, except for **2**, which was done at the microanalytical laboratory at Sun Yat-Sen University in Guangzhou, P. R. China. Samples were vacuum-dried prior to elemental analyses to remove the interstitial solvent molecules of the crystals. Note that this procedure resulted in partial removal of the axial acetonitrile ligands from **4**. Magnetic susceptibility measurements were made on crushed crystalline samples from which the interstitial solvents had been removed by vacuum. The samples were carefully weighed and placed in a plastic bag, which was mounted in a drinking straw and then placed inside a Quantum Design SQUID magnetometer MPMS-XL. Variable temperature data were collected from 2 to 300 K at a field of 1000 G, and the data were corrected empirically for diamagnetism of the sample and the holder. ¹H NMR spectra were obtained on a VXR-300 NMR spectrometer. Mass spectrometry data (electrospray ionization) were recorded at the Laboratory for Biological Mass Spectrometry at Texas A&M University, using an MDS Series Qstar Pulsar with a spray voltage of 5 keV. Visible spectra were obtained on either a Shimadzu UV-2501 PC UV–vis spectrophotometer or a Cary 17D spectrophotometer. Electronic reflectance spectra were obtained in the region from 400 to 1000 nm on a HP 845x UV–visible system with a Labsphere RSA-HP-8453 reflectance accessory.

Syntheses. $\text{Cr}_3(\text{depa})_4\text{Cl}_2$ (2**):** Hdepa (0.45 g, 2.0 mmol) was dissolved in 25 mL of THF. The solution was cooled in a dry ice/acetone bath, and 1.3 mL of 1.6 M CH_3Li in ether was added slowly. The yellow solution was allowed to warm to room temperature, and then was transferred via cannula to a reaction flask containing anhydrous CrCl_2 (0.19 g, 1.5 mmol). The red mixture was stirred at room temperature for 1 h, and then refluxed for 3 h, giving a deep green mixture. The solvent was removed under vacuum, the remaining green-brown solid was extracted with toluene (2×8 mL), and the solution was then layered with hexanes. After 1 week, deep green crystals of $\text{Cr}_3(\text{depa})_4\text{Cl}_2 \cdot 0.5\text{C}_6\text{H}_{14}$ formed. The crystals were collected, washed with hexanes several times, and dried under vacuum. Yield: 0.272 g, 48%. Anal. Calcd for $\text{C}_{39}\text{Cl}_2\text{Cr}_3\text{H}_7\text{N}_{12}$: C, 60.33; H, 6.04; N, 14.30. Found: C, 60.15; H, 5.88; N, 13.99. Mass spectrum, ESI + (m/z): 1130 M^+ . IR (KBr, cm^{-1}): 3751 w, 3448 br, w, 3056 w, 2964 m, 1611 vs, 1532 m, 1473 s, 1424 vs, 1300 m, 1225 w, 1179 m, 1061 m, 1016 s, 928 m, 809 s, 547 w, 436 w. Vis (CH_2Cl_2 solution: λ , nm (ϵ , $\text{M}^{-1}\text{cm}^{-1}$): 664 (900), 608 (1000), 511 (2000), 436 (4000).

$[\text{Cr}_3(\text{depa})_4\text{Cl}_2]\text{I}_3$ (3**):** To a mixture of 80 mg (0.071 mmol) of $\text{Cr}_3(\text{depa})_4\text{Cl}_2$ and 40 mg (0.071 mmol) of ferrocenium triiodide was added 10 mL of dichloromethane. The resulting dark green solution was stirred for 2 h, and then 30 mL of hexanes was added, precipitating a dark green solid and leaving a pale yellow solution which was removed by filtration. The solid was washed with 10 mL of hexanes and redissolved in 10 mL of dichloromethane. This was filtered into a crystallization tube where it was layered with hexanes. Large dark green crystals of $[\text{Cr}_3(\text{depa})_4\text{Cl}_2]\text{I}_3$ formed in about a week. These were collected, washed with hexanes, and dried under vacuum. Yield: 90 mg, 84%. Anal. Calcd for $\text{Cr}_3\text{C}_{36}\text{N}_{12}\text{H}_{64}\text{Cl}_2\text{I}_3$: C, 44.46; H, 4.23; N, 11.11. Found: C, 43.97; H, 4.24; N, 10.73. Mass spectrum, ESI + (m/z): 1130 $[\text{Cr}_3(\text{depa})_4\text{Cl}_2]^+$, ESI – (m/z): 381 I_3^- . IR (KBr, cm^{-1}): 3448 w, br, 2965 w, 2930 w, 1615 s, 1529 w, 1471 m, 1423 vs, 1346

(26) For a recent review of molecular electronics, see: Carroll, R. L.; Gorman, C. B. *Angew. Chem., Int. Ed.* **2002**, *41*, 4378.

(27) Berry, J. F.; Cotton, F. A.; Lu, T.; Murillo, C. A.; Wang, X. *Inorg. Chem.* **2003**, *42*, 3595.

(28) Berry, J. F.; Cotton, F. A.; Murillo, C. A.; Roberts, B. K. *Inorg. Chem.* **2004**, *43*, 2277.

(29) Neuse, E. W.; Loonat, M. S. *J. Organomet. Chem.* **1985**, *286*, 329.

m, 1226 w, 1181 w, 1058 w, 1016 m, 930 m, 859 w, 816 m, 739 w, 551 w, 438 w.

[Cr₃(dpa)₄(NCMe)₂](PF₆)₂ (4): To a flask containing 858 mg (0.946 mmol) of Cr₃(dpa)₄Cl₂ and 661 mg (1.89 mmol) of TlPF₆ was added 25 mL of acetonitrile. After the resulting green mixture was stirred for 4 h, a fine white precipitate was observed. The mixture was filtered through Celite, giving a clear dark olive green solution, which was layered with ether. After diffusion of the ether into the acetonitrile solution, large green block-shaped crystals of [Cr₃(dpa)₄(NCCH₃)₂](PF₆)₂·2CH₃CN formed. These were collected, washed with hexanes, and dried under vacuum. Yield: 824 mg, 72%. Anal. Calcd for C₄₁H_{33.5}N_{12.5}Cr₃P₂F₁₂: C, 42.93; H, 2.94; N, 15.26. Found: C, 42.44; H, 3.29; N, 15.54. IR (KBr, cm⁻¹): 3448 w, br, 2268 w (C≡N), 1608 s, 1551 m, 1468 vs, 1429 vs, 1362 s, 1314 m, 1284 m, 1244 w, 1159 s, 1114 w, 1058 w, 1020 m, 840 vs (PF₆), 766 s, 741 m, 650 w, 557 m, 517 w, 437 w. Vis (CH₃CN solution: λ, nm (ε, M⁻¹ cm⁻¹)): 679 (2000), 561 (1000), 515 (sh, 2000), 435 (sh, 4000).

Cr₃(dpa)₄I₂ (5): In a drybox, 0.105 g (0.087 mmol) of **4** was added to a Schlenk flask. To a second flask was added 0.028 g (0.19 mmol) of NaI that had been powdered and weighed in air. The flask was evacuated and purged with N₂, and 10 mL of freshly distilled MeOH was added to each flask, and then the NaI solution was transferred via cannula to the flask containing **4**. The color darkened, and a crystalline precipitate formed. The mixture was stirred for 1 h. The green solid was collected by filtration and washed with diethyl ether (2 × 20 mL). The solid was dissolved in 12 mL of CH₂Cl₂ and filtered into a Schlenk tube. The green solution was layered with hexanes, and block-shaped crystals were observed the following day. These were collected, washed with hexanes, and dried under vacuum. Yield: 70 mg, 74%. Anal. Calcd for Cr₃C₄₀H₃₂N₁₂I₂: C, 44.05; H, 2.96; N, 15.41. Found: C, 44.63; H, 2.86; N, 15.92. IR (KBr, cm⁻¹): 3448 w, br, 3096 w, 3067 w, 3024 w, 2370 w, 2344 w, 1606 s, 1595 s, 1547 w, 1466 vs, 1426 vs, 1362 s, 1314 m, 1282 w, 1265 w, 1152 m, 1110 w, 1055 w, 1012 w, 916 w, 878 w, 860 w, 763 m, 734 m, 643 w, 537 w, 515 w, 434 w, 420 w.

Cr₃(dpa)₄Br₂ (6): This was synthesized similarly to **5**. IR (KBr, cm⁻¹): 3027 w, 2963 w, 1607 s, 1595 s, 1547 m, 1468 vs, 1429 vs, 1363 s, 1317 m, 1283 w, 1263 m, 1167 m, 1152 m, 1109 m, 1056 m, 1015 m, 917 w, 877 w, 860 w, 802 m, 764 m, 734 m, 702 w, 645 w, 536 w, 516 w, 472 w, 434 w, 419 w.

Cr₃(dpa)₄(NO₃)₂ (7): In air, 0.10 g (0.11 mmol) of Cr₃(dpa)₄Cl₂ and 0.065 g (0.24 mmol) of TlNO₃ were weighed and added to a Schlenk flask which was then evacuated, purged with nitrogen, and then charged with 10 mL of acetone while stirring. After 4 h, some precipitate was visible. The green mixture was filtered over Celite into a Schlenk tube, and the resulting solution was layered with hexanes. After 3 days, small crystals were observed on completion of the diffusion. These were too small for diffraction studies, so the solvents were removed by decantation and then crystals were dried under vacuum. The green crystals were dissolved in 7 mL of CH₂Cl₂ and layered with Et₂O. Block-shaped crystals grew in 2 days. Yield: 23 mg, 21%. Anal. Calcd for Cr₃C₄₄H₄₂N₁₄O₇: C, 51.07; H, 4.09; N, 18.95. Found: C, 51.07; H, 4.05; N, 18.45. IR (KBr, cm⁻¹): 3448 w, br, 3071 w, 3028 w, 2969 w, 2864 w, 2367 w, 2344 w, 1606 s, 1596 s, 1548 w, 1468 vs, 1427 vs, 1361 s, 1305 s, 1155 m, 1109 w, 1016 m, 883 w, 859 w, 819 w, 767 m, 741 w, 647 w, 538 w, 519 w, 437 w.

Cr₃(dpa)₄(BF₄)₂ (8): In air, 0.152 g (0.17 mmol) of Cr₃(dpa)₄Cl₂ was weighed and added to a Schlenk flask with 0.098 g (0.34 mmol) of dried and powdered TlBF₄. The flask was placed under vacuum and purged with nitrogen, and 10 mL of CH₂Cl₂ was added to the flask. After being stirred for 1.5 h, the mixture was filtered over Celite into a Schlenk tube and layered with hexanes for crystallization. Diamond-shaped, dark green crystals were observed within 3 days. Yield: 17 mg, 10%. Anal. Calcd for Cr₃C₄₀H₃₂N₁₂B₂F₈: C, 47.55; H, 3.19; N, 16.64. Found: C, 47.38; H, 3.22; N, 16.45. IR (KBr, cm⁻¹): 3448 w, br, 3072 w, 3035 w, 2963 w, 2672 w, 2603 w, 2491 w, 2368 w, 2344 w, 1607 s, 1597 s, 1550 w, 1468 vs, 1427 vs, 1359 s, 1315 m, 1286 w,

1264 w, 1156 m, 1122 m, 1110 m, 1085 m, 1019 m, 955 w, 928 m, 883 w, 860 w, 805 w, 766 m, 749 w, 649 w, 537 w, 517 w, 436 w, 421 w.

Cr₃(dpa)₄(CN)₂ (9): In a drybox, 0.098 g (0.081 mmol) of **4** was added to a Schlenk flask. Dried and powdered KCN (0.011 g, 0.17 mmol) was weighed in air and added to a second flask, followed by evacuation and purging with N₂. To each flask, 10 mL of MeOH was added while stirring. The solution of KCN was transferred to the Cr₃ flask via cannula. The mixture was stirred for 5 min, after which the solvent was removed under vacuum while heating. The product was extracted from the dried residue with 10 mL of CH₂Cl₂. The extract was filtered over Celite into a Schlenk tube, and the solution was then carefully layered with hexanes. Large dark green block-shaped crystals were observed the following day. Yield: 37 mg, 51%. Anal. Calcd for Cr₃C_{43.5}H₃₅N₁₄Cl₃: C, 51.41; H, 3.47; N, 19.30. Found: C, 51.79; H, 3.60; N, 19.14. IR (KBr, cm⁻¹): 3448 w, br, 3028 w, 2965 w, 2370 w, 2344 w, 2096 w, C≡N, 2063 w, 1606 s, 1595 s, 1546 w, 1467 vs, 1428 vs, 1364 s, 1314 m, 1282 m, 1264 m, 1153 m, 1109 m, 1015 m, 879 w, 859 w, 803 w, 765 m, 735 m, 645 w, 537 w, 517 w, 474 w, 435 w. Mass spectrum, ESI + (*m/z*): 888 (M - H)⁺.

Cr₃(dpa)₄(NCS)₂ (10): In the drybox, 0.076 g (0.063 mmol) of **4** was added to a Schlenk flask. To a second flask was added 0.013 g (0.13 mmol) of dried and powdered KSCN. Next, 10 mL of MeOH was added to each flask while stirring. The contents of the KSCN flask were transferred to the other flask via cannula. After the mixture was stirred for ~15 min, a green precipitate was observed. This was collected by filtration, washed with Et₂O (2 × 10 mL), and dissolved in toluene (12 mL). The resulting green mixture was filtered over Celite into a Schlenk tube, and the solution was layered with hexanes. Crystals grew as long (10 mm +) but very thin needles within a week. Yield: 53 mg, 88%. Anal. Calcd for Cr₃C₄₂H₃₆N₁₄O₂S₂: C, 51.01; H, 3.67; N, 19.37. Found: C, 50.83; H, 3.56; N, 19.37. IR (KBr, cm⁻¹): 3447 w, br, 3071 w, 3028 w, 2963 w, 2368 w, 2342 w, 2028 vs, C=N, 1597 s, 1547 w, 1463 vs, 1425 vs, 1367 s, 1311 m, 1279 w, 1155 m, 1108 w, 1055 w, 1015 m, 916 w, 879 w, 857 w, 802 w, 764 m, 738 w, 645 w, 538 w, 518 w, 434 w. Vis (CH₂Cl₂ solution: λ, nm (ε, M⁻¹ cm⁻¹)): 686 (1000), 614 (1000), 512 (2000), 450 (4000). Mass spectrum, ESI + (*m/z*): 953 M⁺.

Cr₃(dpa)₄(NCO)₂ (**11**) was prepared similarly to **10**,³⁰ and cocrystallized with an oxidized Cr₃⁷⁺ species (**12**). The separation was accomplished manually.³¹

X-ray Crystallography. Crystal data are shown in Table 1. For the previously reported²³ solvates of **1** (1·benzene, 1·toluene, 1·CH₂Cl₂, and 1·THF), the data sets from our archives were re-refined using SHELXL-97³² without any further data processing. For 1·benzene and 1·toluene, the central Cr atoms of each trichromium moiety were removed and replaced by two atoms each with 0.5 occupancy ~0.2 Å in either direction toward the terminal Cr atoms. These atoms were refined with isotropic thermal parameters, and the positions and relative occupancies were allowed to refine with the constraint that the sum of the occupancies for the disordered atoms equal 1. The positions of the central Cr atoms after convergence of least squares refinement were different from the starting positions. Thermal ellipsoid plots of **1** from 1·toluene as obtained in the previously reported refinement and as

(30) Cr₃(dpa)₄(NCO)₂: Anal. Calcd for Cr₃C₄₂H₃₄N₁₄O₃: C, 53.73; H, 3.65; N, 20.89. Found: C, 53.70; H, 3.57; N, 20.45. IR (KBr, cm⁻¹): 3480 w, br, 3071 w, 3027 w, 2966 w, 2367 w, 2344 w, 2175 w, 1605 s, 1594 s, 1547 w, 1466 vs, 1426 vs, 1364 s, 1311 m, 1280 w, 1155 m, 1108 w, 1053 w, 1015 m, 917 w, 878 w, 856 w, 763 m, 739 w, 644 w, 627 w, 557 w, 535 w, 517 w, 434 w.

(31) Cr₃(dpa)₄(NCO)₂ cocrystallized with the oxidized species [Cr₃(dpa)₄(NCO)F]PF₆: IR (KBr, cm⁻¹): 3595 w, 3482 w, br, 3074 w, 3030 w, 2965 w, 2796 w, 2672 w, 2611 w, 2506 w, 2183 vs, 1751 w, 1604 s, 1550 w, 1465 vs, 1427 vs, 1363 s, 1310 m, 1279 w, 1245 w, 1156 m, 1112 w, 1054 w, 1016 w, 919 w, 840 s, 765 m, 740 w, 647 w, 625 w, 557 w, 537 w, 517 w, 438 w. The axial F anion is probably abstracted from a PF₆ anion.

(32) Sheldrick, G. M. *SHELXTL97*; University of Göttingen: Göttingen, Germany, 1997.

Table 1. Crystal Data

compound	1•benzene Cr ₃ (dpa) ₄ Cl ₂ • C ₆ H ₆	1•toluene Cr ₃ (dpa) ₄ Cl ₂ • C ₇ H ₈	1•CH ₂ Cl ₂ Cr ₃ (dpa) ₄ Cl ₂ • CH ₂ Cl ₂	1•ether Cr ₃ (dpa) ₄ Cl ₂ • Et ₂ O	2•0.5hexane Cr ₃ (depa) ₄ Cl ₂ • 0.5hexane	3 [Cr ₃ (depa) ₄ Cl ₂] ₃	4•2CH ₃ CN [Cr ₃ (dpa) ₄ - (NCMe) ₂] (PF ₆) ₂ •2CH ₃ CN	5•CH ₂ Cl ₂ Cr ₃ (dpa) ₄ Cl ₂ • CH ₂ Cl ₂
formula	C ₄₆ H ₃₈ Cl ₂ - Cr ₃ N ₁₂	C ₄₇ H ₄₀ Cl ₂ - Cr ₃ N ₁₂	C ₄₁ H ₃₄ Cl ₄ - Cr ₃ N ₁₂	C ₄₄ H ₄₂ Cl ₂ - Cr ₃ N ₁₂ O	C ₅₉ H ₇₁ Cl ₂ - Cr ₃ N ₁₂	C ₅₆ H ₆₄ Cl ₂ - Cr ₃ I ₃ N ₁₂	C ₄₈ H ₄₄ Cr ₃ - F ₁₂ N ₁₆ P ₂	C ₄₁ H ₃₄ Cl ₂ - Cr ₃ I ₂ N ₁₂
FW	985.78	999.81	992.60	981.80	1175.18	1512.79	1290.93	1175.50
crystal system	orthorhombic	orthorhombic	orthorhombic	monoclinic	tetragonal	tetragonal	monoclinic	orthorhombic
space group	<i>Pna</i> 2 ₁	<i>Pca</i> 2 ₁	<i>Pnn</i> 2	<i>P</i> 2 ₁ / <i>c</i>	<i>P</i> 4̄ <i>n</i> 2	<i>I</i> 4̄ <i>c</i> 2	<i>C</i> 2/ <i>c</i>	<i>Pnn</i> 2
<i>a</i> , Å	18.634(5)	18.475(2)	12.996(2)	16.1062(9)	19.1659(6)	17.929(1)	28.057(2)	13.320(5)
<i>b</i> , Å	29.36(2)	14.965(4)	14.1381(8)	15.8183(9)	19.1659(6)	17.929(1)	10.1744(7)	14.299(6)
<i>c</i> , Å	16.142(3)	16.469(1)	11.331(1)	17.0329(9)	16.080(1)	21.828(3)	22.899(2)	11.460(5)
β, deg	90	90	90	98.471(1)	90	90	124.674(1)	90
<i>V</i> , Å ³	8830(6)	4553(1)	2081.9(4)	4292.2(4)	5906.8(5)	7017(1)	5376.0(6)	2182.8(15)
<i>Z</i>	8	4	2	4	4	4	4	2
<i>d</i> (calc), g cm ⁻³	1.483	1.458	1.583	1.519	1.321	1.432	1.595	1.788
Flack parameter	-0.04(2)	-0.03(3)	-0.08(4)		-0.03(2)	<i>c</i>		0.05(2)
R1, ^a wR2 ^b (<i>I</i> > 2σ <i>I</i>)	0.0540, 0.1203	0.0516, 0.1158	0.0449, 0.1078	0.0522, 0.0913	0.0334, 0.0919	0.0984, 0.2426	0.0320, 0.0872	0.0257, 0.0671
R1, ^a wR2 ^b (all data)	0.0707, 0.1333	0.0646, 0.1251	0.0533, 0.1155	0.0998, 0.1054	0.0388, 0.0992	0.1044, 0.2588	0.0367, 0.0911	0.0282, 0.0692

compound	6•CH ₂ Cl ₂ Cr ₃ (dpa) ₄ Br ₂ • CH ₂ Cl ₂	7•Et ₂ O Cr ₃ (dpa) ₄ (NO ₃) ₂ • Et ₂ O	8•2CH ₂ Cl ₂ Cr ₃ (dpa) ₄ (BF ₄) ₂ • 2CH ₂ Cl ₂	9•CH ₂ Cl ₂ Cr ₃ (dpa) ₄ (CN) ₂ • CH ₂ Cl ₂	10•2benzene Cr ₃ (dpa) ₄ (NCS) ₂ • 2benzene	10•2toluene Cr ₃ (dpa) ₄ (NCS) ₂ • 2toluene	11 Cr ₃ (dpa) ₄ - (NCO) ₂	12•3CH ₂ Cl ₂ [Cr ₃ (dpa) ₄ F- (NCO)]PF ₆ • 3CH ₂ Cl ₂
formula	C ₄₁ H ₃₄ Br ₂ Cl ₂ - Cr ₃ N ₁₂	C ₄₄ H ₄₂ Cr ₃ - N ₁₄ O ₇	C ₄₂ H ₃₆ B ₂ Cl ₄ - Cr ₃ F ₈ N ₁₂	C ₄₃ H ₃₄ Cl ₂ - Cr ₃ N ₁₄	C ₅₄ H ₄₄ Cr ₃ - N ₁₄ S ₂	C ₅₆ H ₄₈ Cr ₃ - N ₁₄ S ₂	C ₄₂ H ₃₂ Cr ₃ - N ₁₄ O ₂	C ₄₄ H ₃₈ Cl ₆ - Cr ₃ F ₇ N ₁₃ OP
FW	1081.52	1034.92	1180.25	973.74	1109.15	1137.20	920.82	1297.54
crystal system	orthorhombic	monoclinic	monoclinic	orthorhombic	monoclinic	orthorhombic	monoclinic	monoclinic
space group	<i>Pnn</i> 2	<i>P</i> 2 ₁ / <i>c</i>	<i>Cc</i>	<i>Pnn</i> 2	<i>C</i> 2/ <i>c</i>	<i>Fdd</i> 2	<i>P</i> 2 ₁ / <i>c</i>	<i>P</i> 2 ₁ / <i>c</i>
<i>a</i> , Å	13.098(1)	16.289(3)	18.844(3)	13.2514(8)	16.956(6)	14.285(1)	13.869(2)	17.310(2)
<i>b</i> , Å	14.203(1)	16.374(2)	17.059(3)	14.1573(8)	18.688(6)	24.356(2)	16.771(3)	16.038(2)
<i>c</i> , Å	11.410(1)	17.373(1)	16.439(3)	11.4203(7)	16.949(6)	31.508(2)	17.083(3)	19.006(3)
β, deg	90	103.624(9)	111.710(3)	90	108.149(6)	90	94.928(3)	90.782(3)
<i>V</i> , Å ³	2122.5(4)	4503.3(9)	4910(1)	2142.5(2)	5104(3)	10 962(1)	3959(1)	5276(1)
<i>Z</i>	2	4	4	2	4	8	4	4
<i>d</i> (calc), g cm ⁻³	1.692	1.526	1.597	1.509	1.444	1.378	1.545	1.634
Flack parameter	0.003(8)		<i>c</i>	0.01(2)		0.01(2)		
R1, ^a wR2 ^b (<i>I</i> > 2σ <i>I</i>)	0.0262, 0.0644	0.0818, 0.1684	0.0530, 0.1472	0.0255, 0.0667	0.0377, 0.0977	0.0332, 0.0824	0.0468, 0.1265	0.0521, 0.1312
R1, ^a wR2 ^b (all data)	0.0319, 0.0673	0.1098, 0.1866	0.0550, 0.1497	0.0281, 0.0685	0.0539, 0.1084	0.0387, 0.0864	0.0613, 0.1361	0.0867, 0.1514

^a R1 = $\sum ||F_o| - |F_c|| / \sum |F_o|$. ^b wR2 = $[\sum [w(F_o^2 - F_c^2)]^2 / \sum [w(F_o^2)^2]]^{1/2}$, $w = 1/\sigma^2(F_o^2) + (aP)^2 + bP$, where $P = [\max(0, F_o^2) + 2(F_c^2)]/3$. ^c Refined as a racemic twin.

obtained by the procedure just described are shown in parts a and b, respectively, of Figure 1. It should be noted that the elongated thermal ellipsoid for the central Cr atom in Figure 1a indicates the presence of this unresolved disorder. The difference between the long and short Cr–Cr distances, $\Delta d_{\text{Cr–Cr}}$, is ~ 0.23 Å. This difference is statistically real because, even in the very worst case, it is >20 times the standard deviation. The occupancies of the central Cr atom positions converged to the following ratios: 65:35 and 57:43 for the two independent molecules in 1•benzene, and 52:48 for 1•toluene.

In the previously reported structure of 1•CH₂Cl₂, the two Cr–Cr distances were constrained to be equal by the crystallographic two-fold axis that passes through the midpoint of the Cr₃ chain. In our re-refinement of this structure, however, the central Cr atom was split into two and each half moved ~ 0.2 Å off of the two-fold axis toward a terminal Cr atom. After several cycles of least squares refinement with an occupancy of 0.5 and an isotropic thermal parameter, the central

half atoms converged to positions about 0.1 Å off of the two-fold axis. Here, the disordered central Cr atom is required to have an occupancy of 0.5 by the crystallographic 2-fold symmetry.

By re-refining the structure of 1•THF similarly, it was found that the central Cr atom did move back to its initial position of 222 symmetry. Attempts were made to crystallize 1 from THF again to get a data set of higher quality, but there were difficulties as discussed later.

For 1•Et₂O, 2•0.5hexane, 3, 4•2CH₃CN, 5•CH₂Cl₂, 6•CH₂Cl₂, 8•2CH₂Cl₂, 9•CH₂Cl₂, 10•2benzene, 10•2toluene, 11, and 12•3CH₂Cl₂, for which structures have not previously been reported, suitable crystals were mounted either on the end of a quartz fiber or on a nylon loop and transferred to the goniometer of a Bruker SMART CCD area detector diffractometer and cooled to -60 °C. Geometric and intensity data were collected using SMART software³³ and were processed using SAINT software³⁴ into SHELX format. Corrections for absorption were

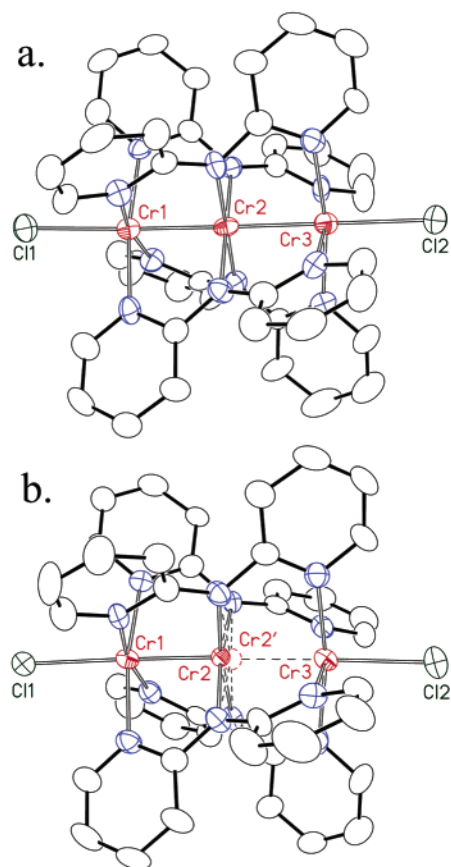


Figure 1. Thermal ellipsoid plot of **1**·toluene (a) as it appears in ref 23 and (b) as reinterpreted here with ellipsoids drawn at the 50% probability level. Solvent molecules and hydrogen atoms have been omitted.

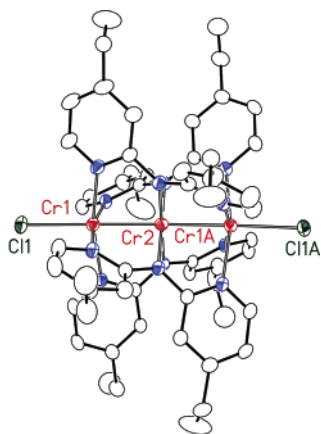


Figure 2. Thermal ellipsoid plot of **2** with ellipsoids drawn at the 30% probability level. Hydrogen atoms have been removed, and only one orientation of the disordered ethyl groups is shown.

applied using SADABS.³⁵ A crystal of **6**·Et₂O was mounted on the tip of a quartz fiber and transferred to the goniometer of a Nonius FAST area detector system. Geometric and intensity data were collected using the software program MADNES³⁶ and processed into SHELX format by the program PROCOR.³⁷ The program SORTAV was used to correct for absorption.³⁸

(33) SMART V5.618 Software for the CCD Detector System; Bruker Analytical X-ray Systems, Inc.: Madison, WI, 1998.

(34) SAINTPLUS, V6.45A Software for the CCD Detector System; Bruker Analytical X-ray System, Inc.: Madison, WI, 1998.

(35) SADABS V2.10. Program for absorption correction using SMART CCD data based on the method of Blessing: Blessing, R. H. *Acta Crystallogr.* **1995**, *A51*, 33.

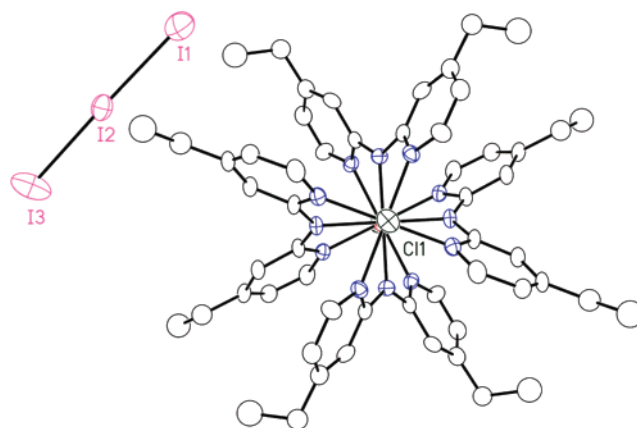


Figure 3. Thermal ellipsoid plot of **3** viewed along the Cr₃ axis with ellipsoids drawn at the 30% probability level. Hydrogen atoms are removed, and only one orientation of the disordered ethyl groups is shown.

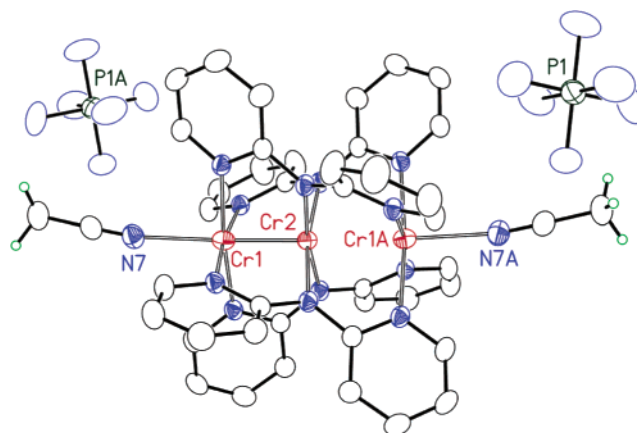


Figure 4. Thermal ellipsoid plot of **4** from **4**·2CH₃CN with ellipsoids drawn at 50% probability. Pyridyl hydrogen atoms and one of the two orientations of the disordered central chromium atom have been omitted for clarity.

In most cases, the space group was determined unambiguously from the systematic absences in the data. For those which were not determined unambiguously, the choice of centrosymmetric versus noncentrosymmetric groups was made on the basis of the intensity statistics of the data and successful structure refinements. The structures were solved either by direct methods or by the Patterson method and refined using SHELXL-97.^{32,39} Crystal data are listed in Table 1, and important interatomic distances are shown in Table 2. For all structures in noncentrosymmetric space groups, the correct choices of polar axes were assured by refinement of the Flack parameter.⁴⁰ Compounds **3** and **8** were refined as racemic twins. Figures 2–6 show thermal ellipsoid plots of compounds **2**, **3**, **4**, **9**, and **10**, respectively.

(36) Pflugrath, J.; Messerschmidt, A. MADNES, Munich Area Detector (New EEC) System, Version EEC 11/1/89, with enhancements by Enraf-Nonius Corp., Delft, The Netherlands. A description of MADNES appears in: Messerschmidt, A.; Pflugrath, J. *J. Appl. Crystallogr.* **1987**, *20*, 306.

(37) (a) Kabsch, W. *J. Appl. Crystallogr.* **1988**, *21*, 67. (b) Kabsch, W. *J. Appl. Crystallogr.* **1988**, *21*, 916.

(38) Program for absorption correction for Enraf-Nonius FAST diffractometer using the method of: Blessing, R. H. *Acta Crystallogr.* **1995**, *A51*, 33.

(39) The refinement of most of the crystal structures presented was routine except with respect to the disordered interstitial solvent molecules were refined with distance constraints on the disordered moieties. In **7**·Et₂O and **8**·2CH₂-Cl₂, in which all of the Cr atoms and the axial ligands are disordered, the two orientations of the molecule were restrained to have a similar geometry, although it should be pointed out that in the case of **8**, the geometry of the molecule is slightly different in the major and minor orientations.

(40) Flack, H. D. *Acta Crystallogr.* **1983**, *A39*, 876.

Table 2. Selected Interatomic Distances for Compounds 1–12

compound	Cr–Cr, Å	Cr···Cr, Å	Cr–N (inner), Å	Cr–N (outer), Å	Cr–L (axial), Å	$\Delta d_{\text{Cr–Cr}}$, Å	Cr1···Cr3, Å
1•benzene	2.227[9]	2.483[9]	2.029[6]	2.118[5]	2.532[2]	0.256[9]	4.710[9]
	2.236[9]	2.481[9]	2.028[6]	2.116[5]	2.544[2]	0.245[9]	4.719[9]
1•toluene	2.24[1]	2.48[1]	2.031[7]	2.123[6]	2.556[2]	0.24[1]	4.718(2)
1•CH ₂ Cl ₂	2.254(4)	2.477(4)	2.027[6]	2.114[5]	2.550(2)	0.223(4)	4.731(2)
1•Et ₂ O	2.249[4]	2.469[4]	2.031[4]	2.115[3]	2.530[1]	0.220[4]	4.717[4]
2•0.5hexane	2.3780(5)	symmetrical	2.022[3]	2.134[3]	2.5122(9)	0	4.7560(5)
3	2.146(8)	2.441(8)	2.03[1]	2.101[9]	2.356(4)	0.295(8)	4.587(8)
4•2CH ₃ CN	2.143(3)	2.464(3)	2.036[4]	2.101[1]	2.339(2)	0.321(3)	4.607(3)
5•CH ₂ Cl ₂	2.184(1)	2.482(1)	2.014[4]	2.114[3]	2.996(1)	0.298(1)	4.666(1)
6•CH ₂ Cl ₂	2.223(1)	2.482(1)	2.026[3]	2.122[2]	2.7364(4)	0.259(1)	4.705(1)
7•Et ₂ O ^a	1.934(5)	2.644(5)	2.036[6]	2.107[7]	2.09(1)	0.712(5)	4.578(5)
					2.30(1)		
8•2CH ₂ Cl ₂ ^a	1.963(5)	2.590(5)	2.034[9]	2.106[6]	2.204(7)	0.627(5)	4.553(5)
					2.347(6)		
9•CH ₂ Cl ₂	2.3700(3)	symmetrical	2.032[2]	2.119[2]	2.284(2)	0	4.7400(3)
10•2benzene	2.234(1)	2.482(1)	2.039[2]	2.113[2]	2.203(2)	0.248(1)	4.716(1)
10•2toluene	2.215(1)	2.465(1)	2.020[3]	2.116[2]	2.203(3)	0.249(1)	4.680(1)
11	2.26[1]	2.48[1]	2.030[4]	2.118[3]	2.177[4]	0.22[1]	4.735(1)
12•3CH ₂ Cl ₂	1.9905(9)	2.576(1)	2.014[3]	2.106[3] (NCO)	2.134(4) (NCO)	0.586(1)	4.566(1)
				2.075[4] (F)	1.868(3) (F)		

^a Bond distances from only the major orientation of **7** and **8** are given. The corresponding distances for the minor orientation have larger esd's and may not be accurate.

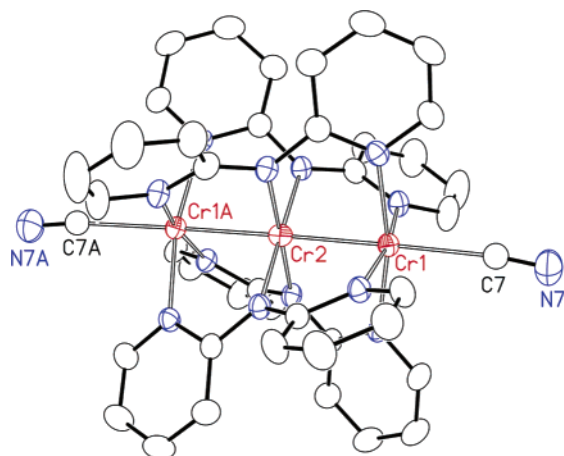


Figure 5. Thermal ellipsoid plot of **9** with ellipsoids drawn at 50% probability. Hydrogen atoms and interstitial solvents have been omitted.

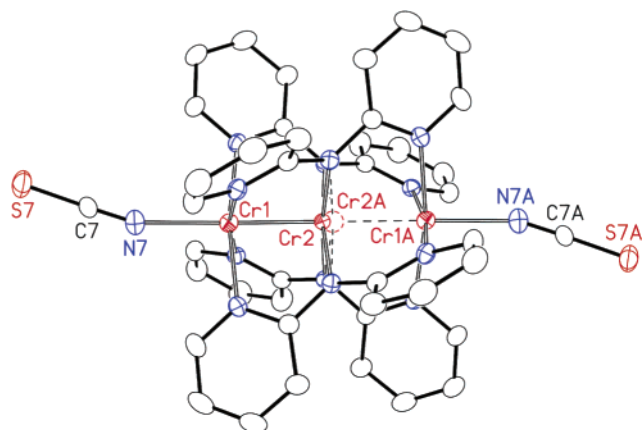
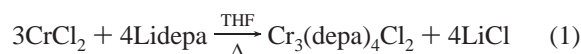


Figure 6. Thermal ellipsoid plot of **10** with ellipsoids drawn at 30% probability. Hydrogen atoms were removed.

3. Results and Discussion

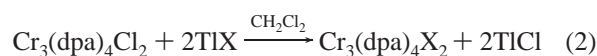
Syntheses. The syntheses of trichromium compounds with the dpa ligand and with the ethyl-substituted homologue (depa) proceeded similarly. Whereas Cr₃(dpa)₄Cl₂ precipitates from the

reaction mixture, reaction of Lidepa and CrCl₂ in a 4:3 ratio in refluxing THF generates Cr₃(depa)₄Cl₂ (**2**) in solution. As already noted for the analogous cobalt⁴¹ and nickel²⁷ compounds, complexes with the ethyl-substituted depa ligand are much more soluble than those of the dpa ligand.



Oxidation of **2** with the easily prepared and mild oxidant ferrocenium triiodide yields the Cr₃⁷⁺ species **3**, similarly to the previously described syntheses of related Cr₃(dpa)₄³⁺ species.⁴²

For the syntheses of Cr₃(dpa)₄X₂ complexes with X other than Cl, two methods are useful. The first is simple metathesis with thallium reagents (eq 2).



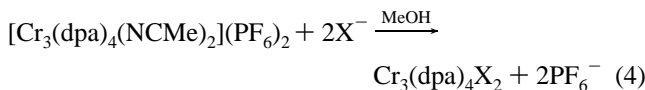
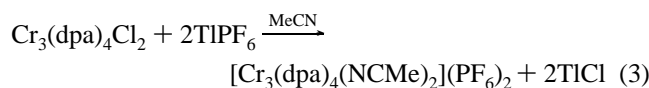
Silver reagents are not used to avoid oxidation. For example, while reaction of **1** with 1 equiv of AgBF₄ yields the unsymmetrical compound Cr₃(dpa)₄Cl(BF₄), 2 equiv of AgBF₄ is enough to oxidize the core to Cr₃⁷⁺.¹⁹ Thus, the nonoxidizing TlBF₄ salt must be used to prepare Cr₃(dpa)₄(BF₄)₂, **8**. An analogous reaction with TlNO₃ yields Cr₃(dpa)₄(NO₃)₂, **7**. Unfortunately, only low yields of **7** and **8** were obtained. This difficulty prompted us to seek another route to Cr₃⁶⁺ complexes with labile axial ligands.

It has been found that reaction of **1** with TIPF₆ in acetonitrile produces [Cr₃(dpa)₄(NCMe)₂](PF₆)₂, **4** (eq 3), in high yield, and this is a useful starting material for the synthesis of other Cr₃(dpa)₄X₂ complexes by addition of X[−], as shown in eq 4. Most Cr₃(dpa)₄X₂ complexes precipitated readily from the MeOH, and those that did not could be extracted from

(41) Berry, J. F.; Cotton, F. A.; Lu, T.; Murillo, C. A. *Inorg. Chem.* **2003**, *42*, 4425.

(42) Clérac, R.; Cotton, F. A.; Daniels, L. M.; Dunbar, K. R.; Murillo, C. A.; Pascual, I. *Inorg. Chem.* **2000**, *39*, 752.

the residue once the MeOH was removed.

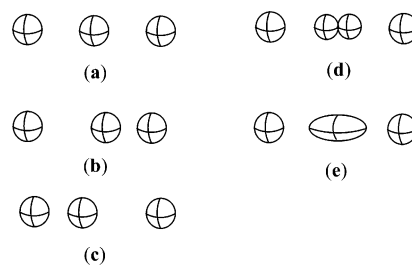


It should be noted that reaction of $\text{Cr}_3(\text{dpa})_4\text{Cl}_2$ with excess NaCN in methanol does not produce $\text{Cr}_3(\text{dpa})_4(\text{CN})_2$, but instead the bright red dinuclear compound $\text{Cr}_2(\text{dpa})_4$ precipitates from the reaction mixture in quantitative yield. This quadruply bonded dichromium complex has been described before.⁴³ Although we did not pursue the isolation of the other products of this reaction, these are probably $\text{Na}_4\text{Cr}(\text{CN})_6$ and NaCl. Because of this, it is necessary to control the stoichiometry carefully and to use **4** in reactions with a stoichiometric amount of NaX as described in eq 4. Compound **4** in solution is very air sensitive, and solutions rapidly turn from green to orange upon exposure to the atmosphere. The reactions described by eq 4 must be carried out under nitrogen to avoid oxidation to Cr_3^{7+} species.³¹ As with the previously reported analogues of nickel, $[\text{Ni}_3(\text{dpa})_4(\text{NCMe})_2](\text{PF}_6)_2$,^{27,44} and cobalt, $[\text{Co}_3(\text{dpa})_4(\text{NCCH}_3)_2](\text{PF}_6)_2$,⁴⁵ **4** is a valuable starting material, useful for the synthesis of $\text{Cr}_3(\text{dpa})_4\text{X}_2$ complexes with various X ligands. While replacement of the axial ligands in trichromium units is also easily carried out by use of the tetrafluoroborate complex $\text{Co}_3(\text{dpa})_4(\text{BF}_4)_2$,⁴⁶ the analogous trichromium tetrafluoroborate complex is much more air sensitive and has been synthesized only in low yields.

Recently, the preparation of $\text{Cr}_3(\text{dpa})_4(\text{NCS})_2$ (**10**) was reported by another group by reaction of CrCl_2 , Hdpa, and KO'Bu, in molten naphthalene followed by stirring with KSCN in a solution open to air for 2 days.⁴⁷ The yield was not given. Furthermore, the reported crystal structure of **10** is not in agreement with the two we report here (vide infra), and the compound was said to be red. Compound **10** as prepared by our method is analytically pure and is dark green. On the basis of the reaction conditions described by the other group and the discussion above, it is likely that the reported method for the synthesis of $\text{Cr}_3(\text{dpa})_4(\text{NCS})_2$ yields a mixture of **10** and the bright red $\text{Cr}_2(\text{dpa})_4$. Thus, to prepare **10** in yields as high as 88% and in good purity, our method involving **4** should be used.

Crystal Structures. Although trichromium EMACs have only recently been discovered, they already pose both experimental and theoretical challenges. As always in science, theoretical efforts cannot succeed without qualitatively and quantitatively reliable data. In dealing with the crystal structures of trichromium EMACs, a particular type of crystallographic disorder often poses an insidious problem. This is represented in Scheme 6. If the trimetal chain is really symmetric (a), the

Scheme 6



thermal displacement ellipsoids representing the atoms will be small and nearly spherical. It is especially important to pay attention to the appearance of the central atom.

If the trimetal chain has one shorter and one longer distance, one might naïvely expect to see a set of ellipsoids as shown in (b) or (c). However, a problem arises because the intermolecular forces that determine the packing of such molecules are short-range and depend on how the outermost atoms of each molecule interact with the outermost atoms of their neighbors. As a result, such molecules tend to occupy the same loci within the limits of detection, and thus their thermal displacement ellipsoids are small and spherical. As for the central atom, it will be an atom having fractional occupancy at each of two sites close to the center (d). Because the vibrational amplitude along the chain direction is equal to or greater than the separation between the loci of the fractional atoms, the normal anisotropic structural refinement procedure will result in the appearance of only one full atom at the center. However, the clue that this is not really the case will be an abnormally elongated shape (prolate spheroid) of the thermal vibration ellipsoid, as shown in (e). When this is seen, it is necessary to carry out a refinement of two partial atoms with coordinates and occupancies as parameters to get a true picture of the unsymmetrical three-atom chain.

The importance of the difference between the two sets of displacement ellipsoids (a) and (e) cannot be overemphasized. If an error is made in this stage of interpreting the structure—that is, taking (e) to be equivalent to (a)—instead of realizing that the structure is a disordered superposition of (b) and (c), there is no hope of finally achieving an understanding of the bonding in the molecule. Here, we provide definitive clarification of this question with regard to compounds **1–12**.

The compound $\text{Cr}_3(\text{dpa})_4\text{Cl}_2$, like its cobalt,⁴⁸ nickel,^{49,50} and copper^{51,52} analogues, crystallizes in many solvates depending on the solvent used for crystallization. We report here a new crystal form of $\text{Cr}_3(\text{dpa})_4\text{Cl}_2$, **1**·Et₂O, which prompted us to reinvestigate the four previously reported²³ structures of **1**: **1**·benzene, **1**·toluene, **1**·CH₂Cl₂, and **1**·THF. The reason for this reinvestigation is that, in **1**·Et₂O, anisotropic refinement of all three Cr atoms revealed that the displacement ellipsoid of the central Cr atom was slightly elongated in the direction of the Cr–Cr vectors as in (e). It could be better refined after being split into two atoms with $\sim 1/2$ occupancy. Thus, the molecule

(43) (a) Cotton, F. A.; Daniels, L. M.; Murillo, C. A.; Pascual, I.; Zhou, H.-C. *J. Am. Chem. Soc.* **1999**, *121*, 6856. (b) Edema, J. J. H.; Gambarotta, S.; Meetsma, A.; Spek, A. L.; Smeets, W. J. J.; Chiang, M. Y. *J. Chem. Soc., Dalton Trans.* **1993**, 789.
 (44) Berry, J. F.; Cotton, F. A.; Murillo, C. A. *Dalton Trans.* **2003**, 3015.
 (45) Clérac, R.; Cotton, F. A.; Dunbar, K. R.; Lu, T.; Murillo, C. A.; Wang, X. *Inorg. Chem.* **2000**, *39*, 3065.
 (46) Clérac, R.; Cotton, F. A.; Jeffery, S. P.; Murillo, C. A.; Wang, X. *Inorg. Chem.* **2001**, *40*, 1265.
 (47) Lin, S.-Y.; Chen, I.-W. P.; Chen, C.-h.; Hsieh, M.-H.; Yeh, C.-Y.; Lin, T.-W.; Chen, Y.-H.; Peng, S.-M. *J. Phys. Chem. B* **2004**, *108*, 959.

(48) Clérac, R.; Cotton, F. A.; Daniels, L. M.; Dunbar, K. R.; Murillo, C. A.; Wang, X. *Inorg. Chem.* **2001**, *40*, 1256.
 (49) Berry, J. F.; Cotton, F. A.; Daniels, L. M.; Murillo, C. A.; Wang, X. *Inorg. Chem.* **2003**, *42*, 2418.
 (50) Aduldecha, S.; Hathaway, B. J. *Chem. Soc., Dalton Trans.* **1991**, 993.
 (51) Berry, J. F.; Cotton, F. A.; Lei, P.; Murillo, C. A. *Inorg. Chem.* **2003**, *42*, 377.
 (52) (a) Wu, L.-P.; Field, P.; Morrissey, T.; Murphy, C.; Nagle, P.; Hathaway, B.; Simmons, C.; Thornton, P. *J. Chem. Soc., Dalton Trans.* **1990**, 3853. (b) Pyrka, G. J.; El-Mekki, M.; Pinkerton, A. A. *J. Chem. Soc., Chem. Commun.* **1991**, 84.

Table 3. Comparison of Previously Reported and Newly Corrected Interatomic Distances for **1**

compound	previously reported Cr–Cr distances, Å ^a	corrected Cr–Cr, Å ^b	corrected Cr···Cr, Å ^b
1 ·benzene	2.296(2), 2.414(2) 2.326(2), 2.390(2) ^c	2.227[9] 2.236[9] ^c	2.483[9] 2.481[9] ^c
1 ·toluene	2.353(2), 2.365(2)	2.24[1]	2.48[1]
1 ·CH ₂ Cl ₂	2.366(1) ^d	2.254(4)	2.477(4)
1 ·THF	2.365(2) ^d	not resolved ^e	
1 ·Et ₂ O		2.249[4]	2.469[4]

^a Data from ref 23. ^b The esd's of these measurements are rather high due to the disorder of the metal atom positions. ^c This structure has two molecules in the asymmetric unit. ^d The two Cr–Cr distances are related by symmetry. ^e See ref 57.

has one short Cr–Cr distance of 2.249[4] Å, and a longer distance, 2.469[4] Å, to the third Cr²⁺ ion.

Reinvestigation of the structures of **1**·benzene, **1**·toluene, and **1**·CH₂Cl₂ by re-refinement of the data sets from our archives showed that these three structures, which were previously reported to be of more or less symmetrical molecules, are also better described as unsymmetrical, as shown in Figure 1. The unusually elongated thermal ellipsoid for the central Cr atom (Figure 1a) has its major axis along the Cr–Cr vector, and this is the best indicator of this type of disorder, which we have noted before in the crystal structures of Cr₃⁷⁺ compounds⁴² and Cr₅¹⁰⁺ compounds.⁵³ It should be mentioned that another Cr₅¹⁰⁺ compound, Cr₅(tpda)₄(NCS)₂⁵⁴ (tpda = tripyridyldiamide), and a heptanuclear chromium compound, Cr₇(tepra)₄Cl₂⁵⁵ (tepra = tetrapyrityldiamide), were reported to have almost evenly spaced Cr–Cr distances even though some of the chromium atoms showed distinctly elongated ellipsoids. We have recently resynthesized the former and shown that the compound is unsymmetrical with alternating long–short–long–short Cr–Cr distances.⁵⁶ In **1**·THF, the molecule crystallizes on a position of 222 symmetry, and attempts to separate the central Cr atom into two components were made, but these were not successful. However, in a reexamination of newly grown crystals of **1**·THF, we have observed a complex diffraction pattern, indicative of twinning. After many unsuccessful attempts at growing better crystals, we do not believe it is possible to obtain a quality structure of **1**·THF, and it will be omitted from further discussions.⁵⁷ A comparison of the previously reported and new interatomic distances for **1** is given in Table 3.

The ethyl-substituted Cr₃(depa)₄Cl₂, **2**, shown in Figure 2, crystallizes in the space group *P4n2* on a position with 2-fold

symmetry, in which the two Cr–Cr distances of 2.3780(5) Å are crystallographically equivalent. The thermal ellipsoid for the central Cr atom in **2**·0.5hexane is not elongated, which strongly suggests that a truly symmetrical molecular structure and not a disordered unsymmetrical structure is present. Although this differs from the results of the re-refined structures of **1**, it is credible, since we have recently reported Cr₃⁶⁺ chains of ligands other than dpa^{58,59} and found that, in some cases, certain equatorial ligands (such as unsymmetrical formamidinates) favor symmetrical Cr₃⁶⁺ chains,⁵⁸ as will be discussed in more detail later.

The more basic depa ligand also allows the Cr₃⁶⁺ chain to be more easily oxidized to Cr₃⁷⁺ (vide infra). The structure of the oxidized species **3** is shown in Figure 3. Although the Cr₃ chain lies on a position of 222 symmetry, it is possible to separate the central Cr atom into two and resolve the asymmetry of the compound. The Cr₃⁷⁺ chain is distinctly unsymmetrical with a short Cr–Cr distance of 2.146(8) Å and a longer distance of 2.441(8) Å to the isolated Cr³⁺ ion, as seen for the previously reported Cr₃⁷⁺ compounds.⁴² It is worth noting that the overall length of the Cr₃ chain (i.e., the distance from Cr1 to Cr3) shortens from 4.7650(5) to 4.587(8) Å upon oxidation. Because the central Cr atom is disordered in two positions, the terminal Cr–N distances do not reflect the differences expected for Cr(II)–N versus Cr(III)–N bond distances, but have an averaged value of 2.101[9] Å. The I₃[−] counteranion is disordered over a site of $\bar{4}$ symmetry and also has unequal I–I distances of 2.848(7) and 2.98(1) Å. In short, both the Cr₃⁷⁺ chain and the I₃[−] chain in this compound are unsymmetrical in the solid state.

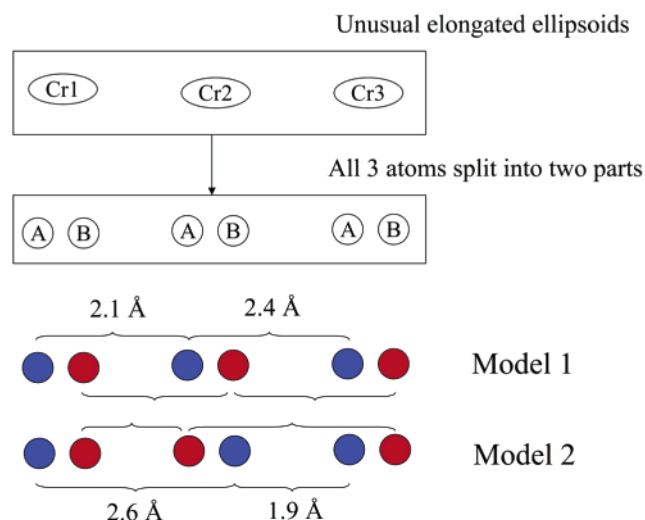
Compounds **5** and **6**, like **1**, crystallize from dichloromethane as monodichloromethane solvates in the noncentric space group *Pnn2*, and again the central Cr atoms in **5**·CH₂Cl₂ and **6**·CH₂Cl₂ may be split into two entities, thus resulting in unsymmetrical molecules with short Cr–Cr distances of 2.184(1) and 2.223(1) Å, and long Cr···Cr separations of 2.482(1) and 2.482(1) Å for **5** and **6**, respectively. The crystal structures of **4**, **10**, and **11** also contain unsymmetrical molecules which are disordered similarly. In a recently reported⁴⁷ crystal structure of **10**, this disorder was not taken into account. The central Cr atom was shown with an elongated thermal ellipsoid and Cr–Cr distances of 2.277(2) and 2.391(2) Å. These do not agree with the ones found here in two independent structures of **10** in which the short Cr–Cr distances are 2.234(1) and 2.215(1) Å and the long Cr···Cr separations are 2.482(1) and 2.465(1) Å for **10**·2benzene and **10**·2toluene, respectively. The disorder of the central Cr atom positions must be taken into account for the proper Cr–Cr bond lengths to be revealed.

Compounds **7** and **8** presented especially severe crystallographic disorder. All three metal atoms in **7**·Et₂O and **8**·2CH₂Cl₂ displayed elongated thermal ellipsoids which suggested that the three “chromium atoms” are really pairs of partial Cr atoms in close proximity. There are two possible models for overlapping Cr₃ molecules, as shown in Scheme 7, depending on how the central Cr atoms are assigned.

- (53) (a) Cotton, F. A.; Daniels, L. M.; Lu, T.; Murillo, C. A.; Wang, X. *J. Chem. Soc., Dalton Trans.* **1999**, 517. (b) Cotton, F. A.; Daniels, L. M.; Murillo, C. A.; Wang, X.; Murillo, C. A. *Chem. Commun.* **1999**, 2461.
- (54) Chang, H.-C.; Li, J.-T.; Wang, C.-C.; Lin, T.-W.; Lee, H.-C.; Lee, G.-H.; Peng, S.-M. *Eur. J. Inorg. Chem.* **1999**, 1243.
- (55) Chen, Y.-H.; Lee, C.-C.; Wang, C.-C.; Lee, G.-H.; Lai, S.-Y.; Li, F.-Y.; Mou, C.-Y.; Peng, S.-M. *Chem. Commun.* **1999**, 1667.
- (56) Berry, J. F.; Cotton, F. A.; Fewox, C.; Lu, T.; Murillo, C. A.; Wang, X., manuscript in preparation.
- (57) Using only the most intense reflections, it was possible to index the pattern to the previously reported tetragonal cell. Yet this does not account for all of the diffraction peaks. More careful inspection revealed that the pattern could be indexed to an orthorhombic cell isomorphous to that in **1**·CH₂Cl₂, which is twinned in four components, all related to one another by 90° rotation about one of the unit cell axes. We believe that the orthorhombic cell is correct and merely simulates the tetragonal symmetry by this complex twinning. Unfortunately, satisfactory refinement of the structure in this *Pnn2* setting was not possible (probably due to incorrect intensity data arising from overlapping reflections from the four twin components), although the THF molecule here is ordered on a position of 2-fold symmetry (disordered over a 222 position in *P4n2*), and the central Cr atom could be refined off the two-fold axis resulting in an unsymmetrical structure. While it is not clear that this twinning necessarily occurred in the previous work on the structure of **1**·THF, we believe this to be so.

- (58) (a) Cotton, F. A.; Lei, P.; Murillo, C. A.; Wang, L.-S. *Inorg. Chim. Acta* **2003**, 349, 165. (b) Cotton, F. A.; Lei, P.; Murillo, C. A. *Inorg. Chim. Acta* **2003**, 349, 173.
- (59) (a) Clérac, R.; Cotton, F. A.; Daniels, L. M.; Dunbar, K. R.; Murillo, C. A.; Zhou, H.-C. *Inorg. Chem.* **2000**, 39, 3414. (b) Cotton, F. A.; Daniels, L. M.; Lei, P.; Murillo, C. A.; Wang, X. *Inorg. Chem.* **2001**, 40, 2778. (c) Cotton, F. A.; Daniels, L. M.; Murillo, C. A.; Wang, X. *Chem. Commun.* **1998**, 39.

Scheme 7

Table 4. Comparison of $M_3(\text{dpa})_4X_2$ Species ($M = \text{Cr, Co, Ni}$)

compound	M–M, Å	M···M, Å	M–L _{ax}	ref
1	2.241[7] ^a	2.478[7] ^a	2.542[2] ^a	this work
<i>s</i> -Co ₃ (dpa) ₄ Cl ₂	2.3369(4) ^b	=	2.4881(8) ^b	22
<i>u</i> -Co ₃ (dpa) ₄ Cl ₂	2.299(1) ^b	2.471(1) ^b	2.399(2) ^b	22
Ni ₃ (dpa) ₄ Cl ₂	2.4313[9] ^a	=	2.333[2] ^a	49
4	2.143(3)	2.464(3)	2.339(2)	this work
[Co ₃ (dpa) ₄ (NCCH ₃) ₂](PF ₆) ₂	2.301[1] ^a	=	2.089[5] ^a	45
[Ni ₃ (dpa) ₄ (NCCH ₃) ₂](PF ₆) ₂	2.374[2]	=	2.049[7]	27
9	2.3700(3)	=	2.284(2)	this work
Co ₃ (dpa) ₄ (CN) ₂	2.3392(2)	=	2.040(2)	46
Ni ₃ (dpa) ₄ (CN) ₂	2.4523(3)	=	2.014(2)	44
10	2.224[1] ^a	2.473[1] ^a	2.203[3] ^a	this work
Co ₃ (dpa) ₄ (NCS) ₂	2.313[1] ^a	=	2.050[5] ^a	46
Ni ₃ (dpa) ₄ (NCS) ₂	2.4285(9)	=	1.988(6)	47
13	2.430[2]	=	2.24[1]	28
Co ₃ (dpa) ₄ (CCPh) ₂	2.344(1)	2.401(1)	2.022[5]	28
Ni ₃ (dpa) ₄ (CCPh) ₂	2.472[1] ^a	=	2.014[8] ^a	28, 44

^a Values are averaged from the different crystal structures reported for this compound. ^b Values are from the 298 K crystal structures.

These two models (and hence the correct Cr–Cr bond distances) would be indistinguishable if the occupancies of the two components were each 50%. Fortunately, for **7**·Et₂O and **8**·2CH₂Cl₂, the occupancy ratios are about 70:30. Thus, one set of three 70% occupied chromium sites and one set of three 30% occupied sites may be chosen, thus allowing for the satisfactory assignment of model 2 for both **7**·Et₂O and **8**·2CH₂Cl₂. Thus, each of these compounds is very unsymmetrical with $\Delta d_{\text{Cr–Cr}} \approx 0.7$ Å, and each has a Cr–Cr quadruple bond distance shorter than 2 Å. It should be noted that the axial ligands in **7** and **8** also display positional disorder since the Cr^{II}–L_{ax} distance from the isolated Cr atom (2.10–2.20 Å) is significantly shorter, as would be expected, than the Cr···L_{ax} distance from the quadruply bonded Cr atom (>2.30 Å).

Crystals of **9**·CH₂Cl₂ are isostructural to **1**·CH₂Cl₂, **5**·CH₂Cl₂, and **6**·CH₂Cl₂ and crystallize in the noncentrosymmetric space group *Pnn*2. Yet compound **9** is crucially different from the others as it contains symmetrical molecules, since the ellipsoid for the central Cr atom is nearly spherical.

It is useful to compare the structures of the Cr₃(dpa)₄X₂ complexes to their Co₃(dpa)₄X₂ or Ni₃(dpa)₄X₂ analogues. For convenience, the relevant data have been collected in Table 4, and, where several structures are known, these data have been averaged except for Co₃(dpa)₄Cl₂. Each Co₃(dpa)₄Cl₂ solvate

has completely different physical properties, and the structure of the molecule changes dramatically depending on the temperature at which the X-ray experiment is done. For simplicity, only the structures of *s*-Co₃(dpa)₄Cl₂·CH₂Cl₂ and *u*-Co₃(dpa)₄Cl₂·2CH₂Cl₂ at 298 K are given in Table 4. Several generalizations can be made about these data. First, unsymmetrical Cr₃⁶⁺ complexes have the shortest M–M distances of all the compounds presented, and this can be attributed to the formation of a localized Cr₂⁴⁺ quadruple bond. Tricobalt complexes are the only other trimetal species with unsymmetrical structures, but of all the symmetrical complexes, tricobalt species have the shortest M–M distances, and one may suppose, perhaps naively, that symmetrical Co₃⁶⁺ chains have a higher bond order. Symmetrical trichromium complexes have Cr–Cr distances of intermediate length. The Ni₃ complexes, which are all symmetric, have the longest interatomic distances, since there are no Ni–Ni bonds in Ni₃⁶⁺ EMACs.

The most notable difference between the Cr₃⁶⁺ complexes and their Co₃⁶⁺ and Ni₃⁶⁺ analogues, however, is that the Cr–L_{ax} distances are uniformly longer by as much as 0.29 Å in the Cr₃⁶⁺ complexes. This difference is large as compared to the difference in the respective atomic radii of Cr, Co, and Ni which differ only by ~0.03 Å.⁶⁰ It might therefore appear that the axial ligands are not bound very tightly, perhaps because Cr–L antibonding orbitals are significantly populated. Despite the long bond lengths to the axial ligands, many of these complexes show the presence of a molecular ion in their mass spectra. Moreover, Co₃⁶⁺ complexes have 21 electrons with which to fill the same molecular orbitals, and there is no elongation of the Co–L distances. Thus, at this time, there is no unambiguous explanation for the long Cr–L distances. It may be noted, however, that a similar elongation occurs in dichromium quadruply bonded species, as shown by the long Cr–L_{ax} distances (in the range from 2.21 to 2.74 Å for various axial ligands) observed in Cr₂(carboxylate)₄(L_{ax})₂ complexes.¹¹ Also, the Cr–NCCH₃ distances of 2.339(2) Å in **4** are almost equal to those in Cr₂(carboxylate)₄(NCCH₃)₂ complexes (2.326[5] Å).¹⁴ This is in marked contrast to the Cr–NCCH₃ distances typically observed for mononuclear Cr(II) species where no Cr–Cr bond is present (~2.07 Å).⁶¹ Since the unsymmetrical Cr₃⁶⁺ complexes can be described as having an isolated Cr₂⁴⁺ quadruple bond, it is reasonable that di- and trinuclear species have similar Cr–L_{ax} bond distances.

It is also useful to compare these trichromium complexes with related Ru₂⁶⁺ compounds having various axial ligands reported by Ren^{62–64} and Bear.⁶⁵ For these Ru₂(L)₄X₂ compounds, there is a dramatic difference depending on whether X is a strong donor ligand (CN or CCPh) or a weaker one (e.g., I or NCNCN).⁶⁴ The former complexes are diamagnetic and have long Ru–Ru distances, whereas the latter are paramagnetic with short Ru–Ru bonds.⁶⁴ It is suggested that in Ru₂(L)₄X₂ complexes with Ru–C bonds (i.e., with X = CN or CCPh), the Ru₂ σ orbitals are used mainly for the formation of the Ru–C

(60) *International Tables for Crystallography*; Wilson, A. J. C., Ed.; Kluwer Academic Publishers: Dordrecht, 1995; Vol. C, p 681.

(61) Henriques, R. T.; Herdtweck, E.; Kühn, F. E.; Lopes, A. D.; Mink, J.; Romão, C. C. *J. Chem. Soc., Dalton Trans.* **1998**, 1293.

(62) Lin, C.; Ren, T.; Valente, E. J.; Zubkowski, J. D. *J. Chem. Soc., Dalton Trans.* **1998**, 571.

(63) Xu, G.; Campana, C.; Ren, T. *Inorg. Chem.* **2002**, *41*, 3521.

(64) Chen, W.-Z.; Ren, T. *Inorg. Chem.* **2003**, *42*, 8847.

(65) Bear, J. L.; Han, B.; Huang, S.; Kadish, K. M. *Inorg. Chem.* **1996**, *35*, 3012.

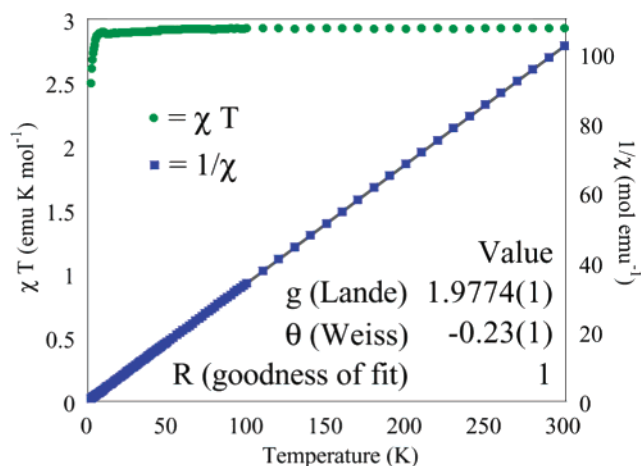


Figure 7. Plots of χT (green circles) and $1/\chi$ (blue squares) versus T for **7**. The solid line along the blue data represents a fit to the Curie–Weiss expression for $S = 2$. The refined parameters are given in the lower right-hand portion of the plot.

Table 5. Magnetic Susceptibility Data for **1–4, 7, 9, 10, and 13**

compound	g (Lande)	θ (Weiss constant, K)	ref
1	2.08	NR ^a	23
2	1.9845(6)	−0.87(6)	this work
3	2.0100(1)	−0.26(1)	this work
7	1.9774(1)	−0.23(1)	this work
9	1.9798(4)	−0.83(4)	this work
10	2.0443(3)	−0.13(3)	this work
13	1.924(2)	−3.2(2)	28

^a NR = not reported.

bonds; thus, in the limit that the σ orbitals are totally used for Ru–C bonding, there is no Ru–Ru σ bond resulting in an unusual $\pi^4\delta^2\pi^{*4}$ configuration.⁶⁴ For these diruthenium systems, the Ru–C bond distances are all less than 2.0 Å. Contrarily, for **9** or **13**, the σ bond probably persists because of the long Cr–C bond distances of ~ 2.20 Å.

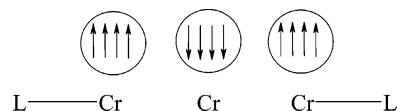
Magnetic Susceptibilities. Compound **1** was previously reported to follow the Curie law with $S = 2$.²³ The magnetic susceptibility data have been measured for **2, 7, 9, 10, and 13**. They are similar and show Curie behavior with four unpaired electrons. The plots of χT versus T for these compounds show a horizontal line at $\chi T \approx 3$ emu K mol^{−1}, which drops at low temperatures. An example is shown in Figure 7, and the others are provided as Supporting Information. This sharp drop in χT at low temperatures is presumably due mainly to zero-field splitting of the quintet ground state, but it may also be influenced by intermolecular antiferromagnetic interactions.

It is useful to fit $1/\chi$ versus T to the Curie–Weiss equation for $S = 2$. Table 5 summarizes the refined g values and Weiss constants (θ) for these compounds. Also given in Table 5 are the refined values for **3** (Cr_3^{7+}) based on a fit assuming $S = 3/2$. All of the g values are close to the free-electron value, and the θ values are in the range from -0.13 to -3.2 K. Some of these compounds (**2, 9, and 13**) contain symmetrical molecules, while the rest are unsymmetrical, and one might have expected that the magnetic behavior would be different for these groups, since the compounds must have dissimilar electronic structures. However, they are not, and the two types of species have four unpaired electrons. The unsymmetrical Cr_3^{6+} chains have smaller Weiss constants (-0.13 to -0.26 K) than those having symmetrical Cr_3^{6+} cores, where θ is at least 3 times as large,

and the value of θ for **13** is larger by an order of magnitude. This difference between the magnetic properties of symmetrical and unsymmetrical compounds may originate in the zero-field splitting which is probably the most important contributing factor to the magnitude of θ . In a symmetrical complex with four unpaired electrons delocalized over three metal atoms, the spin–orbit coupling and hence the zero-field splitting is expected to be larger than for a compound with four unpaired electrons localized on a single metal atom. This corresponds to a more pronounced decrease of χT at lower temperatures for the symmetrical complexes.

It might be questioned whether the symmetrical complexes with Cr–Cr distances over 2.35 Å contain metal–metal bonds at all. For instance, the Cr–Cr distances in **13** of 2.427[2] Å are close to those Ni···Ni separations in $\text{Ni}_3(\text{dpa})_4\text{Cl}_2$ (2.4313[9] Å)⁴⁹ which does not contain Ni–Ni bonds. The difference between **13** and $\text{Ni}_3(\text{dpa})_4\text{Cl}_2$ lies in their electronic structures. If a delocalized electronic structure were to be invoked for the latter, its 24 d electrons would fill and occupy all of the bonding, nonbonding, and antibonding orbitals leaving no net bond. Experimentally, though, $\text{Ni}_3(\text{dpa})_4\text{Cl}_2$ is best described as having a diamagnetic square-planar central Ni^{2+} ion flanked by two terminal high-spin $S = 1$ Ni^{2+} ions which couple antiferromagnetically with each other.⁴⁹ If there were no Cr–Cr bonds in **13**, then the compound would best be treated as containing three high-spin Cr^{2+} ions coupled antiferromagnetically to give an $S = 2$ ground state as shown in Scheme 8. It might then be

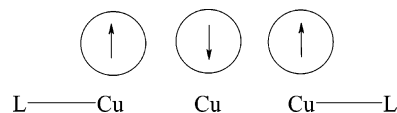
Scheme 8



possible for a higher spin state to be populated at higher temperatures. However, the magnetic susceptibility data for **2, 9, and 13** show no indication of this.

This situation may be contrasted with the magnetic susceptibility data for the tricopper compounds $\text{Cu}_3(\text{dpa})_4\text{Cl}_2$ and $\text{Cu}_3(\text{dpa})_4(\text{BF}_4)_2$ which have $S = 1/2$ ground states arising as in Scheme 9.⁵¹

Scheme 9

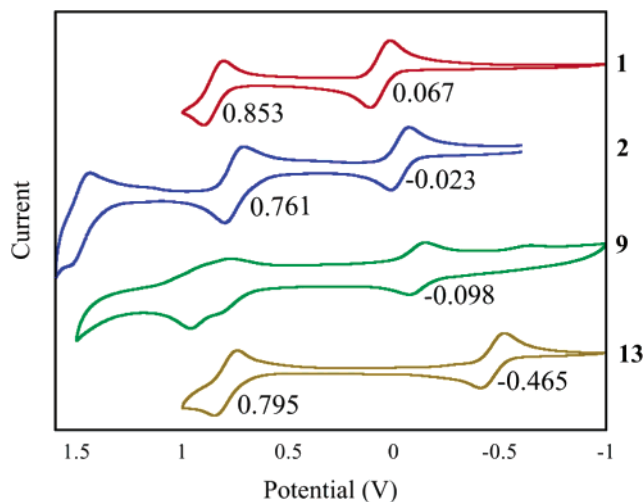


In both of these compounds, which have Cu···Cu separations of 2.47 and 2.40 Å, respectively, population of the $S = 3/2$ state is apparent above ~ 150 K, and the J values from the Hamiltonian $\mathcal{H} = -J(S_A \cdot S_B + S_A' \cdot S_B) - J'(S_A \cdot S_A')$ for these compounds are ~ -400 cm^{−1} (J' values could not be determined).⁵¹

If symmetrical Cr_3^{6+} complexes exist with only antiferromagnetic coupling between the Cr atoms as in Scheme 8, then the J values should be similar to those in $\text{Cu}_3(\text{dpa})_4\text{Cl}_2$ since the pathway for coupling should be the same (superexchange via spin polarization through the dpa ligand). In fact, J for Cr_3^{6+} species would probably be smaller than that for Cu_3^{6+} species since, in the latter, the unpaired electrons reside in the $d_{x^2-y^2}$ orbitals which will have very strong interactions with the ligand

Table 6. Electrochemical Data for Trichromium Compounds

compound	$(E_{1/2})_1$	$(E_{1/2})_2$
1	0.067	0.853
2	-0.023	0.761
4	0.603 (quasi)	not observed
5	0.3 (irreversible)	0.57 (irreversible)
7	irreversible	0.84
9	-0.098	0.9 (irreversible)
10	0.056	0.879
13^a	-0.465	0.795

^a Data from ref 28.**Figure 8.** Cyclic voltammograms of **1**, **2**, **9**, and **13**. The $E_{1/2}$ values are given next to each reversible wave, and the data for **13** are from ref 28.

orbitals. Nevertheless, there is no indication in the magnetic susceptibility data for **2**, **9**, or **13** that any higher spin excited state is being populated, and this militates against the possibility of antiferromagnetic exchange as shown in Scheme 8.

Calculations at the DFT level²⁴ on a symmetrical $\text{Cr}_3(\text{dpa})_4\text{Cl}_2$ structure also have assumed that the π and δ electrons interact via antiferromagnetic coupling. Thus, the only bonding interaction taken into account was the 3-center-3-electron σ bond as discussed above. From these results, the high-spin state ($S = 5$) was calculated to lie $30.8 \text{ kcal mol}^{-1}$ ($>10\,000 \text{ cm}^{-1}$, corresponding to a J value $>500 \text{ cm}^{-1}$) above the ground state. It is unclear to us why such a strong interaction is not considered bonding, and we believe that a correct description of this system must at least include π bonding interactions. Perhaps it would be better to describe the Cr_3^{6+} chain (a 12-electron system) as isolobal to the C_3 chain in allene (also a 12-electron system) with two localized but orthogonal double bonds. We believe that further theoretical work on this system is needed.

Electrochemistry. Oxidation to Cr_3^{7+} species is an important process for all Cr_3^{6+} complexes.⁴² Cyclic voltammetry of the new Cr_3^{6+} complexes was performed to find out how the identity of the bridging or axial ligand changes the ability of the Cr_3^{6+} core to be oxidized. The electrochemical results are shown in Table 6. Compound **1**, whose CV is shown in Figure 8, can be reversibly oxidized twice with $E_{1/2}^{(1)} = 0.067 \text{ V}$ and $E_{1/2}^{(2)} = 0.853 \text{ V}$. The first wave is assigned to the oxidation of the isolated Cr(II) species to Cr(III),⁴² while the second wave is tentatively assigned as oxidation of the Cr_2^{4+} quadruple bond. As seen for $\text{Co}_3(\text{depa})_4\text{Cl}_2$ ⁴¹ and $\text{Ni}_3(\text{depa})_4\text{Cl}_2$,²⁷ both waves for **2** appear at lower potentials than for **1** by $\sim 0.09 \text{ V}$, a result attributed to the increased basicity of the ethyl-substituted depa

ligand. There is also a third wave which is very close to the solvent window which may be assigned to an uncommon $\text{Cr}_3^{8+/9+}$ oxidation.

Replacing the chloride ligands in **1** can drastically change the electrochemical behavior of the Cr_3^{6+} unit, especially with regard to reversibility. While the CV of **10** with axial thiocyanato ligands is very similar to that of **1**, complexes with more weakly donating ligands show less reversible behavior. For example, **6** can be oxidized twice at 0.3 and at 0.6 V, but both processes are irreversible. For complexes having more strongly donating axial ligands, however, a shift in the first oxidation to lower potential occurs, as shown in their CVs (Figure 8). Thus, in the series from Cl to CN to CCPh, the first oxidation potentials for the complexes plummet from 0.067 V for **1** to -0.098 V for **9** to -0.465 V for **13**.²⁸ This may be attributed to the ability of the axial anion to stabilize the isolated Cr^{3+} species in the oxidation product. The second oxidation potentials are not shifted much from their original position, signifying the inability of a more basic axial ligand to stabilize a Cr_2^{5+} unit. Since CN and CCPh are known to be exceptional σ donors, these results suggest that the HOMO of the symmetrical compounds has σ symmetry, as suggested by DFT calculations.²⁴

Spectroscopy. Frequently, paramagnetic species have uninterpretable NMR spectra because the unpaired electrons cause the nuclear spins to have very short relaxation times, thus broadening the signals. It is not uncommon for an NMR spectrum to have no detectable signals for compounds with unpaired spins. Sometimes an interpretation is possible, however, as is the case for $\text{Ni}_3(\text{dpa})_4\text{Cl}_2$ ⁶⁶ and $\text{Co}_3(\text{dpa})_4\text{Cl}_2$.⁶⁷ We thus decided to study the trichromium EMACs by ^1H NMR spectroscopy to see if the spectra could provide information that would allow differentiation between symmetrical or unsymmetrical molecular structures in solution.

The ^1H NMR spectrum of **1** in CD_2Cl_2 solution is not readily interpretable. It features three very broad peaks at -15.2 , -1.4 , and 13.6 ppm which have roughly equal intensity, and which must be due to pyridyl protons. Yet if **1** is symmetrical in solution there should be four resonances, and if it is unsymmetrical there should be eight. The fact that there are only three means that part of the spectrum is unobservable and thus the structure of **1** cannot be assigned as symmetrical or unsymmetrical. The ^1H NMR spectra of **4**, **9**, and **10** are similar to that of **1**.

Interestingly, **2**, which is symmetrical in the solid state, shows a ^1H NMR spectrum in which all of the peaks can be assigned. There are only three pyridyl hydrogen atoms in **2**, and resonances corresponding to these appear at 12.2 , 24.9 , and 27.3 ppm . The ethyl group appears as a triplet at 0.9 ppm for the CH_3 group and a multiplet at 7.2 ppm for the diastereotopic protons of the CH_2 group. This assignment assumes idealized D_4 symmetry for **2** in solution, consistent with what is observed in the solid state.

Compounds having a $\text{Cr}_3(\text{dpa})_4^{2+}$ core are deeply colored and dichroic. An intense green hue by reflected light becomes deep red by transmission through a concentrated solution. The remarkably complicated electronic spectra in the visible region, as shown for **1**, **2**, **4**, **9**, and **10** in Figure 9, display five distinct

(66) Clérac, R.; Cotton, F. A.; Dunbar, K. R.; Murillo, C. A.; Pascual, I.; Wang, X. *Inorg. Chem.* **1999**, *38*, 2655.(67) Cotton, F. A.; Murillo, C. A.; Wang, X. *Inorg. Chem.* **1999**, *38*, 6294.

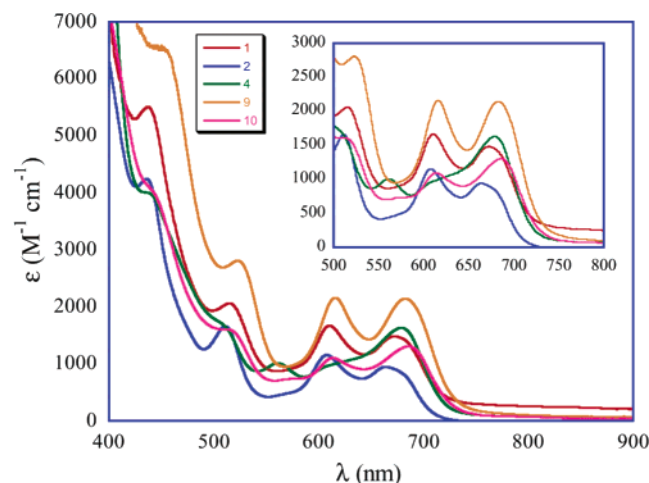


Figure 9. Electronic spectra of **1**, **2**, **4**, **9**, and **10**.

Table 7. Electronic Spectra of Compounds **1**, **2**, **4**, **9**, **10**, and **13**

compound	λ_1 , nm (ϵ , $M^{-1} cm^{-1}$)	λ_2 , nm (ϵ , $M^{-1} cm^{-1}$)	λ_3 , nm (ϵ , $M^{-1} cm^{-1}$)	λ_4 (sh.), nm (ϵ , $M^{-1} cm^{-1}$)
1 (in CH_2Cl_2)	673 (1000)	611 (2000)	515 (2000)	437 (6000)
1 (solid state)	673	612	520	
2 (in CH_2Cl_2)	664 (900)	608 (1000)	511 (2000)	436 (4000)
4 (in CH_3CN)	679 (2000)	561 (1000)	515 (2000)	435 (4000)
9 (in CH_2Cl_2)	683 (2000)	616 (2000)	523 (3000)	455 (7000)
10 (in CH_2Cl_2)	686 (1000)	614 (1000)	512 (2000)	450 (4000)
13 (in benzene)	691 (1000)	625 (1000)	539 (2000)	

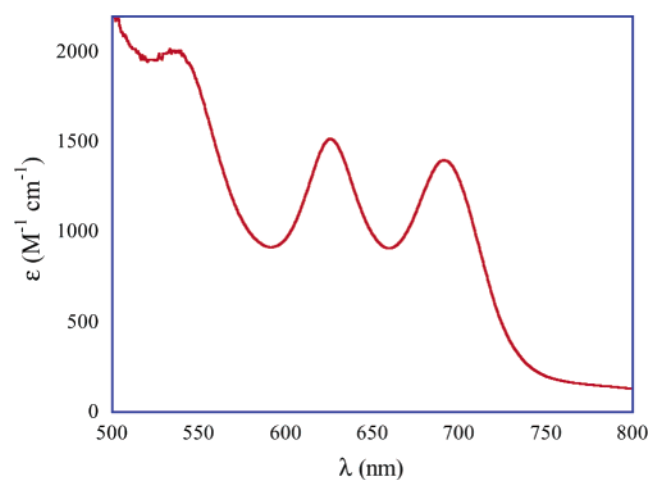


Figure 10. Electronic spectrum in the visible region for **13**.

features: two bands of similar intensity ($\epsilon \approx 1000 M^{-1} cm^{-1}$) at ~ 670 and 610 nm, a much less intense feature at ~ 560 nm, a more intense band at ~ 520 nm, and a very intense band (or shoulder) at ~ 430 nm ($\epsilon \approx 4000 M^{-1} cm^{-1}$). The positions of these bands for **1**, **2**, **4**, **9**, **10**, and **13** are listed in Table 7. While these bands cannot be specifically assigned, their intensities and positions indicate that they are probably d–d transitions. The symmetrical **13**, which is not green but brown, has only three peaks in the range from 500 to 900 nm at 691, 625, and 539 nm (see Figure 10), which are significantly red shifted from their corresponding positions in **1**, **4**, and **10**. The visible

spectrum of **1** taken in the solid state is very similar to the spectrum recorded in solution. In general, quite similar spectra are obtained in solution for all compounds whether they are symmetrical or unsymmetrical in the solid state. Thus, the electronic spectra do not help to distinguish between symmetrical and unsymmetrical species. It should also be noted that **1**, although it contains four unpaired electrons, does not show an EPR spectrum at X-band frequencies at 10 K.

4. Further Comments on the Cr–Cr Bonding in **1**–**13**

Influence of the Axial Ligands. Compounds **1**, **4**–**11**, and **13** have the general formula $Cr_3(dpa)_4X_2$ and differ only in the identity of X. Our previous work indicated that Cr_3^{6+} complexes with X = Cl or $C\equiv CPh$ are symmetrical compounds with chemically equivalent Cr–Cr bond distances, whereas compounds of the type $Cr_3(dpa)_4XY$ with $X \neq Y$ are unsymmetrical with a quadruply bonded Cr_2^{4+} unit and a long interatomic distance to an isolated high-spin Cr^{2+} ion. This expansion of our earlier work shows that some of the previous structural results on different crystalline forms of **1** must be reinterpreted so that **1** is unsymmetrical in the solid state in every case. DFT calculations indicate a symmetrical ground state for **1**,²⁴ which may be a proper description in solution or in the gas phase, even though it is not in the solid state. Even with the concept that **1** lies in a potential energy well which is very shallow with respect to movement of the central chromium atom,²⁴ it is difficult to rationalize the trends in the bond distances presented here, but some important observations can be made.

All of the unsymmetrical Cr_3^{6+} complexes can be described as consisting of a Cr–Cr quadruple bond ($d_{Cr-Cr} < 2.3 \text{ \AA}$) and an isolated high-spin Cr unit. The bond distances of these Cr–Cr quadruple bonds fall into three categories:

$$2.2 \text{ \AA} < d_{Cr-Cr} < 2.3 \text{ \AA} \quad (\text{long})$$

$$2.0 \text{ \AA} < d_{Cr-Cr} < 2.2 \text{ \AA} \quad (\text{medium})$$

$$d_{Cr-Cr} < 2.0 \text{ \AA} \quad (\text{short})$$

From the data in Table 2, it can be seen that good anionic donor ligands (Cl, NCS, NCO) give rise to long Cr–Cr quadruple bonds. Medium length Cr–Cr bonds arise from weaker anionic donor ligands (e.g., iodide) or the neutral acetonitrile ligands. Very weak σ donors such as nitrate and tetrafluoroborate give rise to very unsymmetrical complexes with short Cr–Cr quadruple bonds and an isolated Cr atom which forms a stronger bond to the axial ligand. The axial ligands cyanide and phenylacetylide stabilize symmetrical trichromium chains with equivalent Cr–Cr bond distances $> 2.35 \text{ \AA}$. The common feature of these ligands is that they are exceptionally strong σ donors.

To rationalize the Cr–Cr bonding in these different classes of $Cr_3(dpa)_4X_2$ compounds in terms of molecular orbital theory, three major influences must be taken into account. First of all, three-center bonding must be discussed in relation to the symmetrical compounds. As shown in Scheme 4, the 3-center-3-electron σ bond is the most important concept here. Each of the three combinations of σ orbitals (σ , σ_{nb} , and σ^*) can be displaced in energy by interactions with the axial ligands.

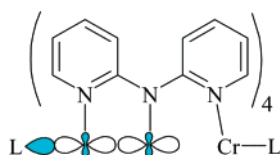
In a Cr–Cr quadruple bond with the configuration $\sigma^2\pi^4\delta^2$, the strongly bonding σ orbital is destabilized by axial donor ligands. The more strongly donating the axial ligand is, the

Table 8. Metal–Metal Separations in Cr₃(L)₄Cl₂ Complexes^a

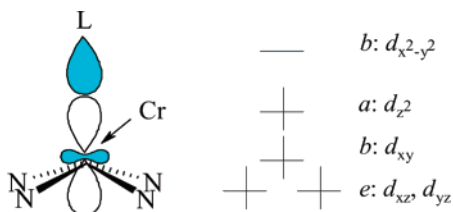
compound	Cr–Cr, Å	Cr···Cr, Å	$\Delta d_{\text{Cr–Cr}}$, Å	Cr1···Cr3, Å	ref
Cr ₃ (dpa) ₄ Cl ₂ ·benzene	2.227[9]	2.483[9]	0.256[9]	4.710[9]	this work
	2.236[9]	2.481[9]	0.245[9]	4.719[9]	
Cr ₃ (dpa) ₄ Cl ₂ ·toluene	2.24[1]	2.48[1]	0.24[1]	4.717(2)	this work
Cr ₃ (dpa) ₄ Cl ₂ ·CH ₂ Cl ₂	2.254(4)	2.477(4)	0.223(4)	4.731(2)	this work
Cr ₃ (dpa) ₄ Cl ₂ ·Et ₂ O	2.249[4]	2.469[4]	0.220[4]	4.717(4)	this work
Cr ₃ (depa) ₄ Cl ₂ ·0.5hexane	2.3780(5)	symmetrical	0	4.7560(5)	this work
Cr ₃ (PhPyBz) ₄ Cl ₂ ·solvents	2.269(1)	2.513(1)	0.244(1)	4.782(1)	58a
Cr ₃ (PhPyF) ₄ Cl ₂ ·CH ₂ Cl ₂	2.4380(8)	2.4602(8)	0.0222(8)	4.8982(8)	58b
Cr ₃ (AniPyF) ₄ Cl ₂	2.4759(7)	2.4789(7)	0.0030(7)	4.9548(7)	58b
Cr ₃ (TolPyF) ₄ Cl ₂ ·2H ₂ O	2.4298(8)	symmetrical	0	4.8478(9)	58b
Cr ₃ (Ph ^F PyF) ₄ Cl ₂	2.460(1)	2.500(1)	0.040(1)	4.960(1)	58b
<i>cis</i> -Cr ₃ (PhPcF) ₄ Cl ₂ ·THF·0.5hexane	2.4743(8)	symmetrical	0	4.9486(8)	58b
(3:1)-Cr ₃ (PhPcF) ₄ Cl ₂ ·THF·0.61Et ₂ O	2.216(1)	2.646(1)	0.430(1)	4.862(1)	58b

^a Brackets represent average values.

longer the Cr–Cr bond distance becomes. In the unsymmetrical trichromium complexes, the Cr–Cr bond has an axial ligand on one side only as shown in Scheme 10.

Scheme 10

These complexes contain, however, another unit which must be taken into account: an isolated square pyramidal Cr^{II} unit, which has the orbital diagram shown in Scheme 11.

Scheme 11

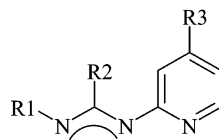
In all cases presented here, the isolated unit is high spin, giving rise to an $S = 2$ ground state for the complexes, and strongly donating axial ligand orbitals of a symmetry (in the group C_4) will destabilize the d_{z^2} orbital.

Thus, the influence of more strongly donating axial ligands is three-fold: strong axial σ donors will destabilize both the Cr–Cr quadruple bond and the isolated high-spin Cr²⁺ ion by raising the Cr–Cr σ bond (shown in Scheme 10) and the d_{z^2} orbital (shown in Scheme 11) in energy. On the other hand, for a delocalized Cr₃ chain, these axial ligands will destabilize the σ_{nb} orbital and to some extent the σ and σ^* orbitals, and this lengthens the Cr–Cr bonds but does not destroy the 3-center bonding in the complex. Thus, very weakly donating axial ligands favor an unsymmetrical Cr₃⁶⁺ chain with short Cr–Cr quadruple bonds. Stronger donors may also give rise to unsymmetrical chains but with a correspondingly longer Cr–Cr quadruple bond. Very strong donors completely destroy the localized Cr–Cr quadruple bond, and the molecule responds to this by employing 3-center bonding which is not destabilized to the same degree as the localized Cr–Cr σ bond. It should be mentioned that no simple Cr₂⁴⁺ complex is known with axial cyanide or acetylide ligands.¹¹ Perhaps the reason is that these

strongly donating ligands will completely break the Cr–Cr bond, but no effort to make such compounds has been reported so the point is moot.

It should also be mentioned here that by employing other bridging ligands several compounds with Cr₃⁶⁺ chains have been synthesized which have no axial ligands at all.⁵⁹ As in the case of complexes with very weak donor ligands, these are all unsymmetrical with very short Cr–Cr quadruple bonds.

Influence of the Equatorial Ligands. Besides the ligand dpa, previous work in this laboratory has employed other polydentate bridging equatorial ligands to stabilize trichromium compounds of the type Cr₃(ligand)₄Cl₂. Some have been unsymmetrical amidinates such as those shown in Scheme 12.⁵⁸

Scheme 12

PhPyBz: R1 = R2 = Ph, R3 = H
 PhPyF: R1 = Ph, R2 = R3 = H
 AniPyF: R1 = *p*-anisyl, R2 = R3 = H
 TolPyF: R1 = *p*-tolyl, R2 = R3 = H
 Ph^FPyF: R1 = *p*-fluorophenylene,
 R2 = R3 = H
 PhPcF: R1 = Ph, R2 = H, R3 = Me

Compound **2**, Cr₃(depa)₄Cl₂, is the first Cr₃⁶⁺ species in which the bridging ligand is a modification of the dipyridylamido ligand. Since all of these compounds (summarized in Table 8) have axial chloride ligands, it is useful to compare them to determine the role of the bridging ligand in the Cr–Cr bonding. As shown in Table 8, the compounds with unsymmetrical formamidinate ligands tend to crystallize with symmetrical structures. The small differences in the two Cr–Cr distances, $\Delta d_{\text{Cr–Cr}}$, despite being statistically meaningful, are chemically insignificant. An exception is (3:1)-Cr₃(PhPcF)₄Cl₂, in which the unsymmetrical Cr₃ chain is thought to derive from the unsymmetrical 3:1 arrangement of the formamidinate ligands.^{58b} By changing from formamidinate ligands to a benzamidinate ligand in Cr₃(PhPyBz)₄Cl₂, the Cr₃⁶⁺ chain becomes distinctly unsymmetrical, with a geometry similar to those unsymmetrical structures of Cr₃(dpa)₄Cl₂. The ethyl-substituted Cr₃(depa)₄Cl₂ is also symmetrical, whereas Cr₃(dpa)₄Cl₂ is not.

One major factor affecting the occurrence of a symmetrical versus an unsymmetrical structure is the basicity of the bridging ligands. We have noted before that the ligand depa is more basic than dpa,⁴¹ because 4-ethylpyridine is more basic than pyridine by 0.8 pK units.⁶⁸ Also, it is reasonable to assume that the phenylpyridylbenzamidinate ligand, PhPyBz, is less basic than phenylpyridylformamidinate, PhPyF, due to the electron-

withdrawing influence of the central phenyl group. Thus, more basic bridging ligands appear to favor symmetrical Cr_3^{6+} chains, whereas less basic ligands favor unsymmetrical compounds. This is probably due to the interaction of the π orbitals of these ligands with the δ orbitals of the trichromium unit, similar to the interactions between ligand π orbitals and $\text{M}-\text{M}$ δ orbitals that lead to the unique properties in complexes of the ligand 1,3,4,6,7,8-hexahydro-2*H*-pyrimido[1,2-*a*]pyrimidine.⁶⁹

Thus, in an unsymmetrical molecule, a more basic ligand will destabilize the localized δ bond of the quadruply bonded Cr_2^{4+} unit through antibonding interactions of the filled π orbitals of the ligand of *b* symmetry in the C_4 point group with the δ bond. However, in a symmetrical molecule (D_4 symmetry), the δ orbitals are essentially nonbonding, so no destabilization of the $\text{Cr}-\text{Cr}$ bonds occurs. Thus, more basic bridging ligands will destabilize the Cr_2^{4+} unit of an unsymmetrical compound and cause a symmetrical structure to be favored.

Oxidation to Cr_3^{7+} Species. All of the previously reported Cr_3^{7+} compounds, whether they contain either the $[\text{Cr}_3(\text{dpa})_4\text{Cl}_2]^+$ cation or cations with radically different axial ligands on either end like compound **12**, are distinctly unsymmetrical. Yet since $\text{Cr}_3(\text{dpa})_4\text{XY}$ compounds are generally very unsymmetrical and we have shown here that neutral $\text{Cr}_3(\text{dpa})_4\text{Cl}_2$ is also unsymmetrical, the question remains: what happens when a symmetrical Cr_3^{6+} complex is oxidized to Cr_3^{7+} ? Will the molecule remain symmetrical, or will it become unsymmetrical, like the $[\text{Cr}_3(\text{dpa})_4\text{Cl}_2]^+$ cations? If the latter is true, then these complexes may find useful applications as molecular switches, since a symmetrical molecule, presumably, would be a better conductor than an unsymmetrical one.

With this question in mind, **2** was oxidized to **3** with ferrocenium triiodide. The structure of **3** is quite unsymmetrical with $\Delta d_{\text{Cr}-\text{Cr}} = 0.295(8)$ Å and the short $\text{Cr}-\text{Cr}$ bond distance of 2.146(8) Å. This is slightly longer than the $\text{Cr}-\text{Cr}$ distance in the $[\text{Cr}_3(\text{dpa})_4\text{Cl}_2]^+$ cation (2.07[1] Å), but nevertheless shows that the electronic structure of $\text{Cr}_3(\text{depa})_4\text{Cl}_2$ changes upon oxidation from a delocalized situation to one having a localized Cr_2^{4+} quadruple bond and an isolated high-spin Cr^{III} ion. We believe that this will be the case for all symmetrical Cr_3^{6+} complexes.

5. Conclusions

This paper presents a wealth of data about compounds containing linear trichromium chains. The crystal structures of solvates of $\text{Cr}_3(\text{dpa})_4\text{Cl}_2$, **1**, which were previously reported to be symmetrical are here shown to be correctly described as unsymmetrical. The change in description results from a meticulous crystallographic analysis of disorder of unsymmetrical molecules of C_4 symmetry which pack in such a way that with single Cr atoms placed (incorrectly) in their averaged positions the molecule appears to have D_4 symmetry. The geometries of all crystalline forms of **1** (except for the twinned **1**·THF) are now consistent with each other, and the $\text{Cr}-\text{Cr}$ distances are essentially the same for each polymorph. Furthermore, previous reports that **1** is symmetric in certain solid-state environments are incorrect. Present results show that the molecule of **1** in

each crystalline compound consists of a quadruply bonded Cr_2^{4+} unit ($\text{Cr}-\text{Cr} = 2.24$ Å) and an isolated high-spin Cr^{2+} species at a longer distance of 2.48 Å. Thus, reported DFT calculations²⁴ on a symmetrical model of **1** may have been performed on a hypothetical molecule, although a symmetric structure of **1** in solution or in the gas phase cannot be ruled out.

Further insight into the bonding in these trichromium compounds has arisen through the study of the properties of a series of $\text{Cr}_3(\text{dpa})_4\text{X}_2$ compounds where the X anions have been weak, intermediate, and strong σ donors: BF_4 , NO_3 , NCCH_3 , Cl, Br, I, NCS, NCO, CN, and CCPh. Use of most of these ligands yields unsymmetrical complexes like **1**, but use of the exceptionally strong donors CN and CCPh result in $\text{Cr}_3(\text{dpa})_4\text{X}_2$ complexes (**9** and **13**) with symmetrical Cr_3 chains. Thus, the $\text{Cr}-\text{Cr}$ bond distances can be tuned by choice of the axial ligand. The range of $\text{Cr}-\text{Cr}$ distances which can be thus obtained is very large (1.93–2.43 Å), although all of the compounds show similar properties. Oddly, the $\text{Cr}-\text{X}$ bond lengths in this series are uniformly longer than the $\text{M}-\text{X}$ distances in corresponding $\text{M}_3(\text{dpa})_4\text{X}_2$ compounds ($\text{M} = \text{Ni}, \text{Co}$) by as much as 0.3 Å. We believe these geometrical features to be clues to the correct description of the electronic structure of these compounds and, more importantly, of all $\text{Cr}-\text{Cr}$ bonded compounds, which have thus far only frustrated theoreticians.¹⁷ The nature of the bridging ligands also has an important impact on the electronic structure of the trichromium chains. The more basic depa ligand was used to synthesize $\text{Cr}_3(\text{depa})_4\text{Cl}_2$, **2**, which has equal $\text{Cr}-\text{Cr}$ distances. Thus, there are two main factors which allow the design of a symmetrical Cr_3^{6+} chain. One is to embrace the Cr atoms with very basic bridging ligands. Another is to employ strong σ -donor axial ligands.

Electrochemical studies of the Cr_3^{6+} complexes have shown that as $\Delta d_{\text{Cr}-\text{Cr}}$ (i.e., the degree of asymmetry) increases, the oxidations to Cr_3^{7+} become less reversible. The symmetrical **2**, **9**, and **13** show reversible $\text{Cr}_3^{6+}/\text{Cr}_3^{7+}$ redox couples which become more accessible as the σ donor strength of the axial ligand increases. This suggests that the HOMO of the symmetrical Cr_3^{6+} chain is σ in character, which is in agreement with the results of DFT calculations. Since oxidation of a complex with a symmetrical Cr_3^{6+} core to one with a Cr_3^{7+} core had not previously been reported, **2** was oxidized to **3** (2^+I_3^-), wherein an unsymmetrical Cr_3^{7+} chain was found (along with an unsymmetrical I_3^- chain). Thus, symmetrical Cr_3^{6+} complexes could be used as molecular switches which can be turned on or off via an applied potential.

Acknowledgment. We thank the NSF for support through a Nanoscale Science and Engineering/NIRT Grant (DMR 0103455) and the Telecommunications and Information Task Force of Texas A&M University. We thank Prof. N. S. Dalal for allowing B.K.R. to participate in this work while training in synthesis at the Laboratory for Molecular Structure and Bonding. J.F.B. thanks the NSF for support in the form of a predoctoral fellowship. We also thank Dr. S. Silber and Dr. V. I. Bakhmutov for helpful discussions on NMR.

Supporting Information Available: Crystallographic data in CIF format and magnetic susceptibility data in PDF format for **2**, **3**, **9**, and **10**. This material is available free of charge via the Internet at <http://pubs.acs.org>.

JA049055H

(68) Martell, A. E.; Smith, R. M. *Critical Stability Constants*; Plenum Press: New York, 1982.

(69) Cotton, F. A.; Gruhn, N. E.; Gu, J.; Huang, P.; Lichtenberger, D. L.; Murillo, C. A.; Van Dorn, L. O.; Wilkinson, C. C. *Science* **2002**, 298, 1971.